AFOSR Scientific Report
AFOSR-TR-72-0814

COMPLETE SOLUTION FOR LIFTING WINGS WITH PARABOLIC TIPS

Peter F. Jordan

NLAE TR 72-034 March 1972

AFOSR Scientific Report
AFOSR-TR-72-0814

COMPLETE SOLUTION FOR LIFTING WINGS WITH PARABOLIC TIPS

Peter F. Jordan

RIAS TR 72-04c March 1972

ABSTRACT: A complete investigation of the solution for lifting wings with parabolic wing tips is presented. All the leading components of the tip pressure singularity are identified. Specific solutions differ from each other by the amplitudes of elements which converge to higher order at the tip; the order of convergence of the specific components also is established. The model used in the analysis is the circular wing in incompressible flow, but the essence of the results is valid for wings of any aspect ratio. For the circular wing, several numerical solutions are given to high accuracy, and several conclusions of immediate technical interest are drawn.

As a by-product of the analysis summation formulas for infinite progressions which involve the logarithm were developed. These are included for completeness of the paper as well as because of their uniqueness.

Research sponsored by the Air Force Office of Scientific Research (AFSC), United States Air Force, under Contract F44620-69-C-0096.

Qualified requestors may obtain additional copies from the Defense Documentation Center; all others should apply to the National Technical Information Service.

UNCLASSIFIED
Security Classification

DOCUMENT CONTROL DATA - R & D
(Security classification of title, body of abstract and indexing annotation must be entered when the overall report is classified)

1. ORIGINATING ACTIVITY (Corporate author)	2a. REPORT SECURITY CLASSIFICATION
MARTIN MARIETTA CORPORATION 1450 SOUTH ROLLING ROAD BALTIMORE, MARYLAND 21227	UNCLASSIFIED 2b. GROUP

3. REPORT TITLE

COMPLETE SOLUTION FOR LIFTING WINGS WITH PARABOLIC TIPS

4. DESCRIPTIVE NOTES (Type of report and inclusive dates)
Scientific Interim

5. AUTHOR(S) (First name, middle initial, last name)
PETER F JORDAN

6. REPORT DATE	7a. TOTAL NO. OF PAGES	7b. NO. OF REFS
March 1972	63	4

8a. CONTRACT OR GRANT NO.	9a. ORIGINATOR'S REPORT NUMBER(S)
F44620-69-C-0096	
b. PROJECT NO. 9781-02	RIAS TR 72-04c
c. 61102F	9b. OTHER REPORT NO(S) (Any other numbers that may be assigned this report)
d. 681307	AFOSR-TR-72-0814

10. DISTRIBUTION STATEMENT
Approved for public release; distribution unlimited.

11. SUPPLEMENTARY NOTES	12. SPONSORING MILITARY ACTIVITY
TECH, OTHER	AF Office of Scientific Research (NAM) 1400 Wilson Boulevard Arlington, Virginia 22209

13. ABSTRACT

A complete investigation of the solution for lifting wings with parabolic wing tips is presented. All the leading components of the tip pressure singularity are identified. Specific solutions differ from each other by the amplitudes of elements which converge to higher order at the tip; the order of convergence of the specific components also is established. The model used in the analysis is the circular wing in incompressible flow, but the essence of the results is valid for wings of any aspect ratio. For the circular wing, several numerical solutions are given to high accuracy, and several conclusions of immediate technical interest are drawn. As a by-product of the analysis summation formulas for infinite progressions which involve the logarithm were developed. These are included for completeness of the paper as well as because of their uniqueness.

DD FORM 1 NOV 68 1473

UNCLASSIFIED
Security Classification

14. KEY WORDS	LINK A		LINK B		LINK C	
	ROLE	WT	ROLE	WT	ROLE	WT
LIFTING SURFACE ANALYSIS						
SUBSONIC FLOW						
PARABOLIC WING TIP						
CIRCULAR WING						
TRANSITION TO SLENDER WINGS						
SUMMATION OF INFINITE PROGRESSIONS						
PSI-FUNCTION						
SINGULARITIES IN POTENTIAL THEORY						

PREFACE

Ludwig Prandtl, concerned about the degree of validity of certain assumptions in his lifting line theory, proposed for W. Kinner (1937) the problem of the circular wing in its exact formulation. Kinner determined overall lift and moment but did not solve the span loading problem; his results are infinite series which appear to diverge at the wing tips. Unfortunately, the answer had to lie in the tip solution, since the key problem is the transition between the lifting line concept (resp. its modern extension, the standard collocation analysis) and the Max Munk concept of the slender wing.

The gap remained until Jordan (1971) showed that the apparent divergence can be overcome. It turned out that, contrary to both the lifting line result and the slender wing result, the correct span loading has a logarithmic component (which, incidentally, causes a vigorous impulse to the vortex trail roll-up).

In the present work, the 1971 analysis is clarified, extended, and brought to its logical conclusion. The complete asymptotic description of the pressure singularity at the wing tip is constructed.

The wing tip pressure singularity is composed of elements of progressively increasing order. Its leading part is general in the sense that the amplitude ratios of its components are fixed numbers. Different solutions are different only in the specific part which consists of components of higher order. Our solution is complete in the sense that the leading general part is completely described, and the orders of the leading components of the specific part also are given. A practical consequence of these analytical results is the ease with which one may calculate specific numerical solutions routinely and to very high accuracy; only a few numbers are required to describe such a solution completely.

Although the main analysis of this paper deals with the circular wing in incompressible flow, the form of the general solution for wings of arbitrary aspect ratio is deducted readily from the results and allows, for example, discussion of the transition between the finite aspect ratio wing and the slender wing model.

LIST OF CONTENTS

I. INTRODUCTION

This paper is concerned with the theory of thin lifting surfaces of finite span ("wings") in linear subsonic flow. The distribution $w(\xi,y)$ of the downwash over the wing surface is given. The given downwash implies a field of flow disturbances and, consequently, a distribution $p(\xi,y)$ of the aerodynamic pressure force which acts on the wing. The specific problem at hand is to find $p(\xi,y)$. Because of analytical difficulties which arise in particular at the wing tips, no complete solution for any problem of this type had been available.

A specific solution, namely, the solution for the planar circular wing in incompressible flow, has been presented recently[1]. The circular wing represents a truly three-dimensional (3-D) problem in that it is well removed from either of the two limit cases for which solutions are known: the two-dimensional (2-D) case of a uniform wing having infinite aspect ratio and the slender wing limit (zero aspect ratio). Also, the circular wing represents a case of a wing having parabolic wing tips. The parabolic wing tip is of particular interest because it fits the usual assumption (which stems from lifting line theory as well as from Munk's minimum drag lemma) that the span loading over any finite wing would be of an elliptic type (i.e., would fit an ellipse at the wing tips). From a technical point of view, the fit should minimize the tip drag; also, because of the fit, one would expect the analytical problem to be less difficult than for any other wing tip shape.

Nevertheless there is a reason why the analytical problem of the parabolic wing tip has remained an intriguing challenge for many years: the assumed fit does not in fact exist. The actual span loading is not of the elliptic type. A corrective (logarithmic) term was derived in Ref. (1).Ø

In the present paper, the analysis of Ref. (1) is generalized and is brought to a logical conclusion. Already the corrective term of Ref. (1) is a general term in the sense that it arises not from the specific downwash w = const. of the planar wing but from a common property of all technically meaningful downwash distributions w. A second such general term is derived in the present paper. Not only do such general terms describe the structure of the general solution, but to know them reduces the numerical work required to calculate specific solutions. (It also greatly reduces the number of numerical values which one has to list to describe a given specific solution.) On the other hand, no such practical benefits arise from

---

Ø The corrective term is in conflict with a standard assumption of collocation analyses. This discrepancy is not of major concern where the goal is to find the pressure load over the main part of the wing, but it markedly affects the roll-up mechanism of the vortex trail.[2]

knowing general terms which are of higher order than the differences between specific solutions. It will be shown that with the determination of the second corrective general term this practical limit is reached.

A sequence of specific solutions has been calculated. These provide insights of technical interest into the mechanism of lifting surfaces.

Although the present analysis deals specifically with the circular wing in incompressible flow, the conclusions regarding the structure of the general solution can be formulated to apply to arbitrary wing planforms with parabolic wing tips in subsonic flow. This is briefly discussed.

Mathematically, the analysis deals with a type of infinite series (a combination of power series and Fourier series) which does not seem to have been explored extensively before. A by-product of our investigation are two sets of formulas of general mathematical interest. These formulas connect the sums of infinite progressions involving the ψ-function (and thus the logarithm) to the Riemann ζ-function. They are derived in Appendix B and seem to be the first formulas of this kind.

II. SURVEY OF THE ANALYTICAL PROBLEM FOR THE CIRCULAR WING

In order to be able to give a survey of the analytical problem at hand, we start this section by describing briefly one aspect of the results of Ref. (1). In the subsequent section, some additional formulas of Ref. (1) are listed (sometimes in modified form resp. supplemented) for easy reference. For brevity, we refer to Eq. (n) of Ref. (1) as (1.n). For further details and for proofs see Ref. (1).

We deal with the circular wing in incompressible flow. It was assumed in Ref. (1) that the given downwash is symmetric and does not contain wing camber. Since no essential aspect of the analytical problem is lost by these restrictions, we retain them here. Thus, using the wing coordinates Fig. 1, we have (1.4)

$$w(\xi,y) \equiv w(y) = w(-y) \tag{1}$$

The pressure distribution $p(\xi,y)$ which arises from $w(y)$ can be described (see Eqs. (9) and (14) below) by an infinite set of coefficients $C_{2\mu}$, $\mu = 0,1,2,3\ldots$. These coefficients are Legendre coefficients of the span load distribution, see Eq. (9a) below. The leading coefficient, C_0, can be determined from the subset $C_{2\mu}$, $\mu = 1,2,3..$, by means of the condition (1.15)

$$\sum_{\mu=0}^{\infty} C_{2\mu} = 0 \tag{2}$$

The subset remains to be determined. We call it the "solving set" for the given downwash w(y).

Ordinarily, the coefficient C_0 is positive, since it measures the total lift: $C_0 = C_L/8$, see (1.6a). Hence the elements of the solving set are ordinarily negative. They can be written in the form

$$- C_{2\nu} = \frac{a_2}{\nu^2} + R_\nu \qquad (\nu \triangleq 1) \qquad (3)$$

Here a_2 is a constant. The remainder R_ν has to converge faster than the leading term:

$$R_\nu = o(\nu^{-2}) \quad \text{as} \quad \nu \to \infty \qquad (3a).$$

Thus the $C_{2\nu}$ converge as ν^{-2}.

We describe the pressure $p(\xi,y)$ by the non-dimensional pressure function $\bar{p} = (1-\xi^2)^{\frac{1}{2}}p/q$ where the factor $(1-\xi^2)^{\frac{1}{2}}$ eliminates the trivial singularities of half-orders at the leading edge (l.e.) and the trailing edge (t.e.). The function $\bar{p}$ is shown for the planar case (w(y)≡1) in Fig. 2. This relief diagram exhibits an interesting type of tip singularity, a singularity which is characteristic for the pressure distribution near any parabolic wing tip. This singularity is produced by the leading term of order ν^{-2} in Eq. (3); its amplitude $\bar{p}_{l.e.}(1)$ is related to the constant a_2 and to the tip value of the local lift coefficient $c_\ell(y)$ by

$$\bar{p}_{l.e.}(1) = 8\sqrt{\pi}\, a_2 = 2c_\ell(1) \qquad (4)$$

see (1.34).

The relations Eq. (4) are valid for any arbitrary set of numbers $C_{2\nu}$ which obey Eqs. (3,3a), resp. for the pressure function $\bar{p}$ which one would calculate from such an arbitrary set. This arbitrary pressure function $\bar{p}$ is finite everywhere. There is thus a temptation to assume that any such set $C_{2\nu}$ would represent the solving set for a technically meaningful lifting surface problem.* However, this is by no means the case.

---

* The pressure distribution p which belongs to $\bar{p}$ has a singularity of order $(1+\xi^2)^{-\frac{1}{2}}$ along the l.e., but this singularity is accepted as "technically meaningful" in linear theory.

One recognizes this as one calculates the induced downwash $w_i(y)$ of $\tilde{p}$ over the wing surface. One finds that $w_i(y)$ will in general diverge toward the wing tip:

$$w_i(y) \rightarrow \pm \infty \quad \text{as} \quad y \rightarrow 1\text{-}0$$

Such divergence is not acceptable: the $w_i(y)$ of the solving set is supposed to equal the given downwash $w(y)$, and any technically meaningful given downwash $w(y)$ is finite everywhere.

In Ref. (1) the fact that $w_i(y)$ has to be finite was used to determine the leading term of the remainder R_μ. Incorporating this term, and making use of Eq. (4), we re-write Eq. (3) as

$$-C_{2\mu} = \left[\frac{1}{\mu^2} - \frac{1}{4\mu^3}\right] \frac{C_\ell(1)}{4\pi} + R_\mu \qquad (\mu \geq 1) \tag{5}$$

The new remainder R_μ here differs, of course, from that of Eq. (3); now $R_\mu = o(\mu^{-3})$. Referring to Eq. (5), we can now describe the structure of the solving set as follows: it consists of a known general term (the term in [ ]-brackets divided by 4π) with an unknown amplitude $C_\ell(1)$, and a remainder R_μ.

Between Eq. (3) and Eq. (5), the infinite set μ^{-3} has been transferred from the remainder into the general term. The first question to which the present paper is addressed is this: is it possible to continue this process, transferring step-by-step further infinite sets (hopefully of successively increasing order of convergence)?

There are indeed further general conditions which are fulfilled, in practice, by all given downwash distributions $w(y)$. Significant for our purpose is the fact that all the derivatives of $w(y)$ are finite (or zero) at the tip. For each successive derivative, this statement translates into an analytical condition of increasing severity for $C_{2\mu}$ and should yield one (or several) additional general sets of successively increasing order. This expectation is in agreement with the fact that such sets describe asymptotic properties of the tip singularity in $\tilde{p}$ which are of increasing order of convergence to zero as the tip is approached (see Ref. 1, Table I).

One is interested to learn more details of the general term because this should reduce the numerical work involved in calculating, for a given downwash $w(y)$, the remainder set R_μ and the amplitude $C_\ell(1)$. On the

other hand, one has to expect to reach a point beyond which to proceed would have little practical purpose. Namely, R_μ must contain, in addition to all the identifiable general sets, a specific signature which describes the given downwash. From the expectation that this specific signature will describe the overall span load distribution rather than its asymptotic tip behavior, one concludes that it will be expressed more by the leading elements ($\mu = 1,2,3...$) of the set R_μ rather than by its tail behavior (the behavior of R_μ as $\mu \to \infty$). Nevertheless, the specific signature has to converge to some order, say to the order O_s, as $\mu \to \infty$. There would be little advantage in knowing details of the general term which converge more rapidly than O_s.

The second problem which has to be addressed thus is to determine the order O_s. The specific signature we define as follows: we select as reference downwash the planar downwash $w_o(y) \equiv 1$. For a given downwash $w(y) \neq w_o(y)$, we define its "void" downwash $w_v(y)$ by

$$w_v(y) = w(y) - Xw_o(y) \tag{6}$$

with the factor X defined by the condition that the tip value $C_{\ell,v}(1)$ of the "void" span loading becomes zero:

$$C_{\ell,v}(1) = C_\ell(1) - XC_{\ell,o}(1) = 0 \tag{6a}$$

The solving set for $w_v(y)$ is then, due to Eq. (5),

$$-C_{2\mu,v} = R_\mu - XR_{\mu,o} \equiv R_{\mu,v} \tag{7}$$

This solving set, which is by definition void of all identifiable general terms, we use as the specific signature of w(y).

We anticipate here briefly the answers to both questions. In (1.18) it had been assumed tentatively that the remainder R_μ of Eq. (5) could be written in the "rational" form

$$R_\mu = \sum_{r=4}^{\infty} (a_r/\mu^r) \tag{8}$$

However, later numerical evaluation of the planar solution, Fig. 2, indicated that Eq. (8) was incomplete: step-by-step determination of the constants a_r

did not converge in a satisfactory manner. Indeed, a review of the analysis confirmed that at least one "missing set" has to be added to Eq. (8). In the analysis of the present paper this missing set is determined. It is $O(\mu^{-4}\log^2\mu)$ and is the third general set (it follows the two general sets which are given in Eq. (5)). To proceed further with this analysis would entail increasing difficulties. Fortunately, the limit of practical interest has already been reached: the order of the fourth general set (appears to be $\mu^{-5}\log^2\mu$ and) is higher than the order O_s of void sets which, from numerical results, appears to be $\mu^{-4}\log\mu$.

The span loading distributions which belong to the elementary sets mentioned in the preceding discussion are illustrated in Appendix A.

A third aspect of the problem, also discussed in this paper, are the numerical methods required to obtain a specific solution. For the reference downwash $w_0(y)$, one determines $C_\ell(1)$ by truncating the given infinite linear system to N equations, matching the solution with the known general terms, and extrapolating to (1/N) = 0. For additional solutions, one determines X (rather than $C_\ell(1)$) in a simpler process. After the remainder R_μ has been determined, its leading terms are extracted; one is then left with a final remainder set $\bar{\bar{R}}_\mu$ which converges very rapidly. The numerical procedure is self-checking since the leading coefficient C_0 is calculated directly and the result must fulfill Eq. (2).

In the present paper, three additional solutions are presented numerically. Thus one has available a three-fold variety of solutions by linear superposition.

III. REFERENCE FORMULAS

The formula for the non-dimensional pressure function $\tilde{p} = (1-\xi^2)^{\frac{1}{2}}p/q$ is (1.5)

$$\tilde{p} = -\frac{4}{(1-y^2)^{\frac{1}{2}}}\left[\sum_{\mu=0}^{\infty} C_{2\mu} r^{2\mu}\cos 2\mu\phi + \sum_{\lambda=0}^{\infty} C_{2\lambda+1} r^{2\lambda+1}\sin(2\lambda+1)\phi\right] \tag{9}$$

The local lift coefficient is (1.6)

$$C_\ell(y) = \frac{2\pi}{(1-y^2)^{\frac{1}{2}}}\sum_{\mu=0}^{\infty} C_{2\mu} P_{2\mu}(y) \tag{9a}$$

and the position of the local center of pressure is (1.7)

$$\xi_\ell(y) = -\frac{\pi}{C_\ell(y)} \sum_{\lambda=0}^{\infty} (2\lambda+1) C_{2\lambda+1} \bar{P}_{2\lambda}(y) \tag{9b}$$

The $P_{2\kappa}(y)$ and $\bar{P}_{2\lambda}(y)$ are systems of orthogonal polynomials. The former are the Legendre polynomials, the latter their derivatives (Gegenbauer or ultraspherical polynomials), normalized such that

$$P_{2\kappa}(\pm 1) = \bar{P}_{2\lambda}(\pm 1) = 1 \qquad \text{(all } \kappa, \lambda) \tag{10}$$

Thus

$$\bar{P}_{2\lambda}(y) = \frac{1}{(\lambda+1)(2\lambda+1)} \frac{d}{dy} P_{2\lambda+1} \tag{11}$$

The two sets of unknown coefficients in Eq. (9), the $C_{2\kappa}$ and the $C_{2\lambda+1}$, are fully interdependent. We introduce the abbreviation

$$\bar{\lambda} \equiv \lambda + \tfrac{1}{2} \tag{12}$$

Then (1.13) reads

$$C_0 = \frac{1}{\pi} \sum_{\lambda=0}^{\infty} \frac{C_{2\lambda+1}}{\bar{\lambda}} \quad ; \quad -C_{2\kappa\neq 0} = \frac{2}{\pi} \sum_{\lambda=0}^{\infty} \frac{\bar{\lambda} C_{2\lambda+1}}{\kappa^2 - \bar{\lambda}^2} \tag{13}$$

We have available also the reversed form (1.19) of Eq. (13):

$$C_{2\lambda+1} = \frac{2}{\pi\bar{\lambda}} \sum_{\kappa=1}^{\infty} \frac{-\kappa^2 C_{2\kappa}}{\kappa^2 - \bar{\lambda}^2} \tag{14}$$

(Note that the system Eqs. (13) fulfills Eq. (2) for any arbitrary set $C_{2\lambda+1}$.)

Usually, the span loading $C_\ell(y)$ is of more immediate concern than the center of pressure $\xi_\ell(y)$ or the complete pressure function $\bar{p}$. Hence the set $C_{2\mu}$ would appear to be of more immediate interest than the set $C_{2\lambda+1}$. However, Eq. (9a) takes the form (0/0) as $y \to 1$; the important tip value $C_\ell(1)$ is thus not immediately given by the set $C_{2\mu}$.

For this tip value we have the formula (1.22b)

$$C_\ell(1) = 8 \sum_{\lambda=0}^{\infty} \bar{\lambda}\, C_{2\lambda+1} \tag{15}$$

This formula has two interesting consequences. One, consider an arbitrary set R_μ which obeys Eq. (3a) (for instance, any finite set R_μ is eligible). According to Eq. (4), this set R_μ does not contribute to $C_\ell(1)$ (i.e., the tip value of its pressure function $\tilde{p}$ is zero). From R_μ, calculate the set R_λ which corresponds to R_μ by means of Eq. (14). From Eq. (15) follows

$$\sum_{\lambda=0}^{\infty} \bar{\lambda}\, R_\lambda = 0 \tag{15a}$$

for all such sets R_λ.

Two, using Eq. (15) in Eq. (9b) to determine the tip value of the pressure center function, we obtain, noting Eq. (10)

$$\xi_\ell(1) = -\pi/4 \tag{16}$$

for any pressure distribution (at least so if $C_\ell(1) \neq 0$). This result is in agreement with the prediction of slender wing theory for the planar elliptic wing. As an illustration, the pressure center function $\xi_\ell(y)$ for the planar circular wing is shown in Fig. 3. (The planar span loading is shown in Fig. A3).

The given downwash w(y) enters the analysis in the form of its set of Gegenbauer coefficients w_s (1.39)[Ø]

$$w(y) = \sum_{s=0}^{\infty} (s+1)(2s+1) w_s \tilde{P}_{2s}(y) \tag{17}$$

Ø We use here the notation w_s in place of the notation $\bar{w}_s$ of Ref. 1.

For example, for the planar wing (i.e., for our reference downwash $w_o(y)$) we have

$$w_o = 1 \quad ; \quad w_{s\neq 0} = 0 \quad \text{if} \quad w(y) \equiv w_o(y) \equiv 1 \tag{17a}$$

The set of given downwash coefficients w_s and the unknown set $C_{2\mu}$ are interrelated by the infinite linear system

$$w_s = \frac{1}{2}\sum_{\mu=0}^{\infty}\left[\frac{1}{\mu+\bar{s}} + \frac{1}{\mu+\bar{s}+\frac{1}{2}} - \frac{2}{\mu-\bar{s}}\right] C_{2\mu} \tag{18}$$

see (1.12) with (1.37). The notation

$$\bar{s} \equiv s + \tfrac{1}{2}$$

is here used. It corresponds to the notation $\bar{\lambda}$, Eq. (12); in fact, the two indices, s and λ, play rather similar roles in the analysis (as we will see shortly).

The system Eq. (18) is a convenient basis for our analysis because of the relative simplicity of its matrix. It is directly equivalent to the (less convenient) original Kinner system, Eq. (60) of Ref. 3. The alternate system

$$w_s = \pi\sum_{\lambda=0}^{\infty} c_\lambda^s C_{2\lambda+1} \tag{19}$$

see (1.14), relates the given set w_s to the unknown set $C_{2\lambda+1}$. This system is preferable for numerical work. It converges well because its matrix c_λ^s differs little from the unit matrix (see Table IIIb of Ref. 1); on the other hand, the c_λ^s are too complicated for convenient analytical treatment (see Table II of Ref. 1).

IV. THE OPERATOR S_0

Using operator notation, we can write Eq. (18) as

$$w_s = S(C_{2\mu}); \qquad C_{2\mu} = S^{-1}(w_s) \tag{20}$$

Our problem would be solved if we could find an explicit form for the reversed operator S^{-1}. Realistically, we cannot expect to find this explicit form in spite of the relatively simple form of S. However, we can determine the salient features of S^{-1}.

The operator S would be still simpler if the summand $\frac{1}{2}$ in the denominator of the second term of its matrix would be zero. Indeed, when $(\mu+s)$ is large, this $\frac{1}{2}$ would appear to be negligible. Actually, as we will see, all the complications which make our analytical problem so interesting are caused by this $\frac{1}{2}$.

Separating out the complication we have for Eq. (18) the form

$$w_s = 2\bar{s}\sum_{\mu=0}^{\infty}\frac{-C_{2\mu}}{\mu^2-\bar{s}^2} + \frac{1}{2}\sum_{\mu=0}^{\infty}\left[\frac{1}{\mu+\bar{s}+\frac{1}{2}} - \frac{1}{\mu+\bar{s}}\right]C_{2\mu}$$

$$= \qquad S_0(C_{2\mu}) \quad + \quad S_1(C_{2\mu}) \tag{21}$$

Elimination of C_0 by means of Eq. (2) yields

$$S_0(C_{2\mu}) = (2/\bar{s})\sum_{\mu=1}^{\infty}\frac{-\mu^2 C_{2\mu}}{\mu^2-\bar{s}^2} \tag{21a}$$

$$S_1(C_{2\mu}) = \frac{1}{2}\sum_{\mu=1}^{\infty}\left[\frac{1}{\bar{s}(\mu+\bar{s})} - \frac{1}{(\bar{s}+\frac{1}{2})(\mu+\bar{s}+\frac{1}{2})}\right]\mu\, C_{2\mu} \tag{21b}$$

Of these two operators, S_0 is dominant in Eq. (21); S_1 is of higher order. With S_0 we are already familiar, and we also know already its reversed operator S_0^{-1}: we can write Eq. (14) as

$$C_{2\lambda+1} = (1/\pi)S_0(C_{2\mu}) \quad ; \quad C_{2\mu} = \pi S_0^{-1}(C_{2\lambda+1}) \tag{22}$$

and can read S_0^{-1} directly by comparing Eq. (22) with Eq. (13).

It follows that we possess already a first order approximate solution, namely, the solution which arises when we set $S_1 \equiv 0$. The set $C_{2\mathfrak{K}}$ can then be calculated from the given set w_s by means of Eq. (20), and the set $C_{2\lambda+1}$ is equivalent with the set w_s since both sets arise from $C_{2\mathfrak{K}}$ by means of the same operator (setting $S_1 \equiv 0$ is equivalent with replacing the matrix c^s_λ in Eq. (19) by the unit matrix from which, in fact, c^s_λ does not differ much). The brief table which follows illustrates the degree of approximation which is reached in this manner for our reference case, Eq. (17a). The first line of the table gives the formula for each coefficient, the second and third lines give the (rounded-off) numerical values, approximative and correct:

coefficient	C_0	C_1	$-C_2$	C_3	$-C_4$	C_5	$-C_6$
approx.	$2/\pi^2$	$1/\pi$	$4/3\pi^2$	0	$4/15\pi^2$	0	$4/35\pi^2$
	0.2026	0.3183	0.1351	0	0.0270	0	0.0116
correct	0.2238	0.3496	0.1446	0.0041	0.0307	0.0014	0.0135

(23)

One sees that the error made by setting $S_1 \equiv 0$ is of the order 10%.[Ø]

Because of the thus illustrated importance of the operator S_0, we set out to investigate its properties in some detail. Since our results will be accurate relations between the sets $C_{2\lambda+1}$ and $C_{2\mathfrak{K}}$ but only approximate relations between w_s and $C_{2\mathfrak{K}}$, we will write our analysis in terms of $C_{2\lambda+1}$ (however, we will later use these results in discussing the relations between w_s and $C_{2\mathfrak{K}}$).

We use the notation $E_{\mathfrak{K}}$ for any one of the elementary sets of which the solving set $-C_{2\mathfrak{K}}$ may be composed. We do not stipulate that $E_{\mathfrak{K}}$ has to be a rational set (i.e., $E_{\mathfrak{K}} = \mathfrak{K}^{-r}$) but assume, on the basis of Eq. (3) and of numerical experience, that $E_{\mathfrak{K}}$ is a progression in $\mathfrak{K}$ which converges to zero smoothly as $\mathfrak{K} \to \infty$. We use the integer r to describe the range of convergence between $\mathfrak{K}^{-r}$ (included) and $\mathfrak{K}^{-r+1}$ (excluded), writing

$$E_{\mathfrak{K}} = \mathfrak{K}^{-r} g_{\mathfrak{K}} \qquad (r \geq 2) \qquad (24)$$

with $g_{\mathfrak{K}} = o(\mathfrak{K})$ but not $o(1)$. If $E_{\mathfrak{K}}$ is a rational set we have $g_{\mathfrak{K}} \equiv 1$; we may also have, for example, $g_{\mathfrak{K}} = \log^n \mathfrak{K}$ or $g_{\mathfrak{K}} = \mathfrak{K}^2$.

The contribution to $C_{2\lambda+1}$ which arises from $E_{\mathfrak{K}}$ by means of Eq. (14) we denote by $C_{2\lambda+1,E}$; thus

---

Ø See also Appendix D.

$$\pi C_{2\lambda+1,E} = (2/\bar{\lambda}) \sum_{\kappa=1}^{\infty} \frac{g_\kappa}{(\kappa^2-\bar{\lambda}^2)\kappa^{r-2}} \tag{25}$$

The sum on the right we take apart by means of the identity

$$\frac{(2/\bar{\lambda})}{(\kappa^2-\bar{\lambda}^2)\kappa^{r-2}} = -(1/\bar{\lambda}^{r+1}) \sum_{\nu=2}^{r-2} \left[1 + (-)^{r-\nu}\right] \left(\frac{\bar{\lambda}}{\kappa}\right)^\nu$$

$$+ (1/\bar{\lambda}^r)\left\{\frac{1}{\kappa-\bar{\lambda}} - \frac{1}{\kappa} - (-)^r \left(\frac{1}{\kappa+\bar{\lambda}} - \frac{1}{\kappa}\right)\right\} \tag{26}$$

Terms with ν arise if $r \geq 4$. Summation of these terms in Eq. (25) does not pose any difficulty[∅] and leads to rational elementary sets $\bar{\lambda}^{-(r-\nu+1)}$ in $C_{2\lambda+1}$, with $(r-\nu+1)$ odd and ≥ 3. More interesting is the final term on the right of Eq. (26). For its contribution we use the following abbreviation:

$$\pi C_{2\lambda+1,E} = \ldots + (1/\bar{\lambda}^r)\, O_{\kappa,\bar{\lambda}}(g_\kappa)$$

Thus

$$O_{\kappa,\bar{\lambda}}(g_\kappa) = \sum_{\kappa=1}^{\infty} \left\{\frac{1}{\kappa-\bar{\lambda}} - \frac{1}{\kappa} - (-)^r \left(\frac{1}{\kappa+\bar{\lambda}} - \frac{1}{\kappa}\right)\right\} g_\kappa \tag{27}$$

From the point of view of analytical difficulties, the operator $O_{\kappa,\bar{\lambda}}(g_\kappa)$ forms the nucleus of the operator S_0.

The details of the reversed operator S_0^{-1} are similar to those of S_0. Corresponding to Eq. (24), we write E_λ for the elementary sets of $C_{2\lambda+1}$ and

$$E_\lambda = \bar{\lambda}^{-t} g_\lambda \qquad (t \geq 3) \tag{28}$$

∅ If $g_\kappa \equiv 1$, summation leads to the Riemann ζ-function. If g_κ is more complicated, it may be necessary to use Eq. (B2).

From Eqs. (13) and (22)

$$-\pi C_{2\kappa,E} = 2\sum_{\lambda=0}^{\infty} \frac{g_\lambda}{(\kappa^2-\bar{\lambda}^2)\bar{\lambda}^{t-1}} \qquad (\kappa\neq 0) \tag{29}$$

An identity similar to Eq. (26) is used to transform this sum. Its terms with β produce rational elementary sets in $C_{2\kappa}$. There remains a final operator which is similar to the operator $0_{\kappa,\bar{\lambda}}(g_\kappa)$:

$$-\pi C_{2\kappa,E} = \ldots + (1/\kappa^t) 0_{\bar{\lambda},\kappa}(g_\lambda)$$

with

$$0_{\bar{\lambda},\kappa}(g_\lambda) \equiv \sum_{\lambda=0}^{\infty} \left\{ \frac{1}{\bar{\lambda}} - \frac{1}{\bar{\lambda}-\kappa} + (-)^t \left(\frac{1}{\bar{\lambda}} - \frac{1}{\bar{\lambda}+\kappa} \right) \right\} g_\lambda \tag{30}$$

The two 0-operators, Eqs. (27) and (30), are readily executed in the case of rational elementary sets (i.e., $g_\lambda \equiv 1$ resp. $g_\lambda \equiv 1$). They then lead into the realm of the psi (digamma) function. One finds

$$0_{\bar{\lambda},\kappa}(1) = \left\{ \begin{matrix} 4L_\kappa \\ 0 \end{matrix} \right\} \text{ if } t \text{ is } \left\{ \begin{matrix} \text{even} \\ \text{odd} \end{matrix} \right\} \tag{31}$$

with

$$L_\kappa = 1 + \frac{1}{3} + \frac{1}{5} + \ldots + \frac{1}{2\kappa-1} = \frac{1}{2}\left[\psi(\kappa+\tfrac{1}{2}) - \psi(\tfrac{1}{2}) \right]$$

$$\rightarrow \tfrac{1}{2}(\log\kappa+\gamma) + \log 2 + 1/48\kappa^2 + \ldots. \tag{31a}$$

and

$$0_{\kappa,\bar{\lambda}}(1) = \left\{ \begin{matrix} (1/\bar{\lambda}) \\ -4L^*_\lambda \end{matrix} \right\} \text{ if } r \text{ is } \left\{ \begin{matrix} \text{even} \\ \text{odd} \end{matrix} \right\} \tag{32}$$

where

$$L^*_\lambda = L_\lambda + (1/4\bar{\lambda}) - \log 2 \tag{32a}$$

The significant observation here is that the 0-operators can produce logarithmic elements from rational elements E_ν resp. E_λ.

If we apply the preceding results to the tentative assumption, Eq. (8), that only rational elements ν^{-r} occur in $C_{2\nu}$, we find that the corresponding elementary contributions $C_{2\lambda+1,E}$ have the following form:

$$\pi C_{2\lambda+1,E} = (A_3^r/\bar{\lambda}^3) + (A_5^r/\bar{\lambda}^5) + (A_7^r/\bar{\lambda}^7) + \ldots \qquad (33)$$

The factors A_t^r are given by the following matrix:

	A_3^r	A_5^r	A_7^r	A_9^r
r=2	1	0	0	0
3	$4L_\lambda^*$	0	0	0
4	$2\zeta(2)$	1	0	0
5	$-2\zeta(3)$	$-4L_\lambda^*$	0	0
6	$-2\zeta(4)$	$-2\zeta(2)$	1	0
7	$-2\zeta(5)$	$-2\zeta(3)$	$-4L_\lambda^*$	0

(33a)

As expected, this matrix contains logarithmic elements. It follows a simple law and is easily extended; also, it is easily reversed.

Conversely, no logarithmic elements can arise if the operator S_0^{-1} is applied to Eq. (33) to regain the elements of $C_{2\nu}$. This explains, see Eq. (31), why only terms with t odd occur in Eq. (33). Interesting is the observation that the operator $0_{\bar{\lambda},\nu}(g_\lambda)$ even eliminates the logarithm from the elements with L_λ^*. To this observation we will return later.

The main result of the preceding investigation of the operators S_0 and S_0^{-1} is that their nuclei are the two 0-operators. A stimulus for investigating the latter further will arise when we consider the complete relations between the sets $C_{2\nu}$ and w_s. Before we turn to this task, let us utilize Eq. (33a) to take a look at the actual solutions, the sets $C_{2\nu}$ and $C_{2\lambda+1}$, for our reference case Eq. (17a).

Let G_ν be the negative of the general term in the [ ]-bracket of Eq. (5):

$$G_0 = + \left[\zeta(2) - \zeta(3)/4\right]$$

$$G_\nu = - \left[\nu^{-2} - \nu^{-3}/4\right] \qquad (\nu \neq 0) \qquad (34a)$$

In Fig. 4, the ratio $C_{2\mu}/G_\mu$ is plotted over μ. For $\mu \to \infty$, this ratio should converge towards $C_1(1)/4\pi \approx 0.12677$. Indeed, after an initial disturbance around $\mu = 1$, convergence is both rapid and smooth.

From Eq. (33), the set G_λ which arises from G_μ is

$$G_\lambda = \left[1 + L^*_\lambda\right]/\pi\tilde{\lambda}^3 \qquad (\text{all } \lambda) \tag{34b}$$

The ratio $C_{2\lambda+1}/G_\lambda$ is also plotted in Fig. 4. There is again smooth convergence, but convergence is now slow. Indeed, all the elements μ^{-r} contribute elements $O(\lambda^{-3})$ to $C_{2\lambda+1}$, see Eq. (33a). Thus, while the components $\lambda^{-3}\log\lambda$ should have corresponding amplitudes in $C_{2\lambda+1}$ and G_λ, already the components $O(\lambda^{-3})$ are likely to be different. Slowness of convergence is an obvious consequence.

A final remark: the formulas of this section can be used to derive certain summation formulas of mathematical interest. This is discussed in Appendix B.

V. THE DOWNWASH CONDITIONS

In view of the normalization Eq. (10), it follows from Eq. (17) that the downwash coefficients w_s must converge $o(s^{-3})$ if the tip value $w(1)$ is to be finite. If one differentiates Eq. (17) once, one finds that the derivatives of the $\bar{P}_{2s}$ are of order s^2 at the tip; hence in order that $w'(1)$ be finite, the w_s must converge $o(s^{-5})$. Further differentiations impose further convergence conditions of increasing severity. However, as already indicated, there will be no need for us to drive our analysis beyond $O(s^{-4})$.

We have to use Eq. (20) in order to translate the convergence conditions for w_s into conditions for $C_{2\mu}$. At first, we make again the tentative assumption that $C_{2\mu}$ is composed of rational sets E_μ, Eqs. (6), (8). For these sets, we know already approximate elements $w_{s,E}$, namely, the elements $\pi C_{2\lambda+1,E}$ of Eqs. (33), (33a). (We have to replace λ by s, of course.) To these we have to add as corrections the contributions of the operator S_1. As we do this, the regular form of Eq. (33a) is lost, and there is then no longer an advantage in using the abbreviations $\tilde{s}$ and L^*_s. Therefore we write our results in terms of s and $\log s$:

$$w_{s,E} = \frac{1}{2}\sum_{\nu=3}^{\infty}\left[(\log s + \gamma)B^r_\nu + C^r_\nu\right]/s^\nu \qquad (s \neq 0) \tag{35}$$

It turns out that the matrix of coefficients B^r_ν is (about) a triangular matrix, with zeros below a zigzag line along its diagonal. The matrix C^r_ν is a full matrix. Of the two, we will use explicitly only the following coefficients:

	B^r_3	C^r_3	B^r_4
r=2	-1	+2.5	2.25
r=3	-4	$-\gamma(2)$	7.5
r≥4	0	$-[4\gamma(r-2) + \gamma(r-1)]$	0

(35a)

Both matrices, B^r_ν and C^r_ν, must have their basis in the matrix A^r_ν, Eq. (33a). Specifically the mechanism which produces B^r_ν is as follows: this matrix must arise from the log-terms $-4L^*_\lambda$ in Eq. (33a). For example, the coefficient B^3_3 corresponds directly to A^3_3. From this, contributions to $B^3_4, B^3_5, \ldots$ arise in two ways. One, from developing the factor, λ^{-3} in Eq. (33), s^{-3} in the case of $w_{s,E}$, in terms of powers $s^{-3}, s^{-4}, \ldots$. Two, from the operator S_1.

The mechanism is the same if r=2, in principle at least, even though there is no log-term for r=2 in Eq. (33a). The point is that in principle there is a log-term A^2_2. Its factor is zero because now r is even in Eq. (32). But Eq. (32) does not apply to the operator S_1. In consequence, S_1 creates non-zero higher order coefficients $B^2_3, B^2_4, B^2_5, \ldots$.

The mechanism for all r odd is similar to that for r=3, and for r even similar to that for r=2. The result is an almost triangular matrix B^r. The first non-zero coefficients on successive lines r are $B^2_3, B^3_3, B^4_5, B^5_5, B^6_7$ ... .[∅]

By a similar mechanism, a full matrix C^r_ν arises from the constant coefficients in Eq. (33a). Because of this, it is readily possible to fulfill successively the conditions that the rational terms $s^{-3}, s^{-4}, \ldots$ in w_s should have the factor zero. Combine Eqs. (5), (8) to read

$$-C_{2\kappa} = \sum_{r=2} (a_r/\kappa^r) \quad \text{so that} \quad w_s = \sum_{r=2} (a_r w_{s,E}) \tag{36}$$

∅ This is as described in the text which precedes (1.42). Regrettably, the manner in which the order of the remainder terms are written in both (1.42) and (2.21) is incorrect. Both equations should be corrected to agree with Eq. (35a).

One simply has to use a sufficient number of elementary sets $\varkappa^{-r}$ and has to determine their amplitudes a_r such that the conditions

$$\sum_{r=2} a_r C_\nu^r = 0 \tag{36a}$$

are fulfilled for all required values ν.

Conversely, it is not possible to extract more detailed conditions for the a_r from Eq. (36a). Hence, in what follows we can disregard the rational terms as neither causing complications nor providing useful information.

Specific conditions arise from the log-terms, however. First, the factor to the terms $s^{-3}\log s$ is zero[Ø], from Eq. (35a), if and only if

$$a_3 = -a_2/4 \tag{37}$$

This result is already incorporated into Eq. (5).

In order to proceed beyond this result of Ref. 1, we have to eliminate next the term $s^{-4}\log s$. Here we encounter an obstacle. Because of Eq. (37) we have now, due to Eq. (35a),

$$w_s = (3/16)\ a_2\ s^{-4}\log s + \ldots \qquad (s \neq 0) \tag{38}$$

This term is different from zero because, in general, $a_2 = C_\lambda(1)/4\pi \neq 0$. No further set is available in Eq. (35a) to cancel this term.

The inescapable conclusion is that Eq. (38) requires an additional elementary set in $C_{2\varkappa}$, a set that is "foreign" to the rational sets $\varkappa^{-r}$ which are represented in Eq. (35a). Applied to this "missing" set, the operator S must produce a contribution which cancels the leading term in Eq. (38) but must not contain lower order terms (disregarding lower order rational terms).

Ø We omit the γ of Eq. (35) for simplicity. If we wish, we may consider γ as part of the rational term.

VI. THE MISSING SET E^*_κ

The task of finding the missing elementary set would appear to imply that one has to try various likely sets, apply the operator S, and hope to obtain a result suitable to cancel the term Eq. (38). Since for transcendental sets the required summation formulas are not usually available, the task as thus described would appear to be formidable. Fortunately, we have available an argument that reduces the same task to a direct form which, furthermore, requires only the performance of analytical integrations.

In view of Eqs. (26/7), we write the missing set as

$$E^*_\kappa = \kappa^{-4} g_\kappa \tag{39}$$

The operator S_0 produces the following contribution to $C_{2\lambda+1}$

$$\overline{\Pi}\, C_{2\lambda+1,E^*} = -2\zeta_g(2)/\bar{\lambda}^3 + O_{\kappa,\bar{\lambda}}(g_\kappa)/\bar{\lambda}^4 \tag{39a}$$

where

$$\zeta_g(r) = \sum_1^\infty \frac{g_\kappa}{\kappa^r}$$

Assume that we can find g_κ such that the result of the 0-operator in Eq. (39) produces $\log\lambda$ as leading term.[∅] Then the corresponding contribution of the operator S_1 will be of the general order λ^{-5}; this contribution is thus not here of interest. Hence we can use the same 0-operator for w_s; the leading terms here are thus found to be

$$w_{s,E^*} = -2\left[\zeta_g(2) + \tfrac{1}{2}\zeta_g(3)\right]/\bar{s}^3 + s^{-4}\log s + \ldots \tag{39b}$$

∅ The logarithmic sets L_κ and L^*_λ which we used earlier were defined for all κ and all λ; in particular, $L_0=0$ and $L^*_0 = \frac{1}{2} - \log 2$. Just as we used $\log s$ instead already in Eq. (35), we use henceforth also $\log\lambda$ even though $\log 0$ does not exist. This formal procedure simplifies the analysis, and it is justified because we are concerned only with the asymptotic behavior as s resp. κ resp. $\lambda \to \infty$. It is readily shown that in this respect the formal analysis leads to the correct result.

The log-term in Eq. (39b) can be used to cancel the term Eq. (38).

Further, since we had to use only the 0-operator of S_0, not of S_1, we can reverse the process. Again disregarding rational sets, we have for the missing set from Eq. (30), since $g_s = g_t/\pi$,

$$g_\kappa = 0_{\bar{s},\kappa}(\log s)/\pi^2 \qquad (t = 4) \tag{40}$$

Equation (40) puts the task of finding the missing set into a direct form. This form still involves inconvenient infinite summations over progressions which involve log s. However, again because we are only interested in the leading term, we can deal with these summations by the method of corresponding integrals. (Essentially, this means using only the leading term on the right of Eq. (B2).)

With t=4, we have from Eqs. (30), (40) formally

$$\pi^2 g_\kappa = \sum_{s=0}^{\infty} \left(\frac{2}{\bar{s}} - \frac{1}{\bar{s}-\kappa} - \frac{1}{\bar{s}+\kappa} \right) \log s \tag{41}$$

This sum, after some rearrangement, including folding of its middle term, becomes

$$2\sum_{s=0}^{\kappa-1} \frac{\log s}{s+\frac{1}{2}} - \sum_{s=0}^{\kappa-1} \frac{1}{s+\frac{1}{2}} \log \frac{\kappa+s}{\kappa-s-1} - \sum_{s=\kappa}^{\infty} \frac{1}{s+\frac{1}{2}} \log (1-(\kappa/s)^2)$$

The corresponding integral of the second of these three sums is

$$\int_{\frac{1}{2}}^{\kappa-\frac{1}{2}} \log \frac{\kappa-\frac{1}{2}+x}{\kappa-\frac{1}{2}-x} \frac{dx}{x} = \int_{(2\kappa-1)^{-1}}^{1} \log \frac{1+u}{1-u} \frac{du}{u} = \frac{\pi^2}{4} + O(\kappa^{-1}) \tag{42a}$$

The integral which corresponds to the last sum is

$$\int_{\kappa}^{\infty} \log(1-(\kappa/x)^2) \frac{dx}{x+\frac{1}{2}} = \int_0^1 \log(1-u^2) \frac{du}{u(1+u/2\kappa)} = -\frac{\pi^2}{12} + O(\kappa^{-1}) \tag{42b}$$

Neither contribution is here of interest. The leading contribution arises from the first sum:

$$2\int_0^{\mu-1} \frac{\log x}{x+\frac{1}{2}}\,dx = 2\int_{\frac{1}{2}}^{\mu-\frac{1}{2}} \log(u-\tfrac{1}{2})\,\frac{du}{u} = \log^2\mu + O(1) \qquad (42c)$$

As we had to expect, the leading contribution is not a rational set. Also, note that this contribution arises as $s \to \mu$; clearly our formal procedure was justified.

We can now list the sets (leading terms only) which belong to E^*_μ in w_s (from Eq. (39b)), $C_{2\mu}$ and $C_{2\lambda+1}$:

w_s, E^*	$-C_{2\mu}, E^*$	$C_{2\lambda+1}, E^*$
$\frac{\log s}{s^4}$	$\frac{\log^2\mu}{\pi^2\mu^4}$	$\frac{\log\lambda}{\pi\lambda^4}$

(43)

This list completes the task which was set by Eq. (39). We use w_s, E^* to cancel the undesirable term on the right of Eq. (38) and arrive at a more detailed form of Eq. (5):

$$-C_{2\mu} = \left[\frac{1}{\mu^2} - \frac{1}{4\mu^3} - \frac{3\log^2\mu}{16\pi^2\mu^4}\right]\frac{C_\mu(1)}{4\pi} + R_\mu \qquad (\mu \geq 1) \qquad (44)$$

To the new set E^* in Eq. (44) belongs, because of Eq. (43), a set in $C_{2\lambda+1}$ which is not contained in Eq. (33a). This term was indeed found in a numerical analysis of the set $C_{2\lambda+1}$, Fig. 4.

Equation (44) essentially completes the task of describing the structure of the solving set $C_{2\mu}$. It disproves the tentative assumption Eq. (8) and implies that to proceed beyond Eq. (44) would require a more involved analysis. In particular, in using the method of corresponding integrals for E^* we neglected the higher order terms which we would then need. Fortunately, as already mentioned, there is no practical need to drive the analysis any further.

We round off this discussion of the sets E^* by showing that the relation between them, Eq. (43), can also be derived by applying the method of corresponding integrals in reversed order.

From Eqs. (27) and (43)

$$\pi^2 w_{s,E^*} = \ldots + (1/s^4) \sum_{\kappa=1}^{\infty} \left(\frac{1}{\kappa - \bar{s}} - \frac{1}{\kappa + \bar{s}} \right) \log^2 \kappa \tag{45}$$

By rearrangement, the sum becomes

$$\frac{\log^2(2\bar{s})}{\bar{s}} + \sum_{\kappa=1}^{s} \frac{1}{\kappa - \frac{1}{2}} \left[\log^2(s+\kappa) - \log^2(s-\kappa+1) \right]$$

$$+ \sum_{\kappa=s+2}^{\infty} \frac{1}{\kappa - \frac{1}{2}} \left[\log^2(\kappa+s) - \log^2(\kappa-s-1) \right]$$

The single term is of no interest and can be dropped. The corresponding integrals for the sums are

$$\int_{\frac{1}{2}}^{\bar{s}-1} \left[\log^2(\bar{s}+x) - \log^2(\bar{s}-x) \right] \frac{dx}{x} + \int_{\bar{s}+1}^{\infty} \left[\log^2(x+\bar{s}) - \log^2(x-\bar{s}) \right] \frac{dx}{x}$$

Setting $x=u\bar{s}$ in the first, $ux=\bar{s}$ in the second and combining, we arrive at the following integral

$$2 \int_0^1 \left[2 \log \bar{s} + \log\left(\frac{1}{u} - u\right) \right] \log \frac{1+u}{1-u} \frac{du}{u}$$

after the limits of the two integrals have been replaced by their values for $s \to \infty$. We have here the integral Eq. (42a), multiplied by 4 log $\bar{s}$, and a further integral which is O(1) and not here of interest. Inserting in Eq. (45), we confirm Eq. (43).

VII. INTERPRETATION

Since the solving sets $C_{2\mu}$ converge with increasing slowness as μ increases, a lengthy tabulation would be required should one wish to communicate a given numerical solution without knowing the structure of $C_{2\mu}$, Eq. (44). Because of Eq. (44), one has to list only the number $C_{\lambda}(1)$ plus the much faster converging set R_{μ}. We refer to the problem of determining the structure as the "inner problem" and to the problem of calculating $C_{\lambda}(1)$ as the "outer problem". With the latter we will deal in the next section and conclude the discussion of the former in the present section.

First we collate our results, Eqs. (31), (33a) reversed, (43) for the operator $O_{\bar{s},\mu}$. For this purpose let

$$w_s = \bar{s}^{-t} g_s \quad \text{and} \quad -C_{2\mu} = \mu^{-t} g_{\mu} / \bar{\mu}^2$$

Again only the leading terms of each set are listed:

g_s	g_{μ}, t even	g_{μ}, t odd
1	$2 \log \mu$	0
$\log s$	$\log^2 \mu$	-1/2

(46)

In general, the g_{μ} are $O(\log^n \mu)$ and are thus within the convergence range defined for g-sets. In all these cases, neither O-operator alters the general order of convergence, i.e., r=t. The two exceptions are borderline cases, $g_s=1$ with t odd, and $g_{\mu}=1$ with r even, see Eq. (32).

The operator $O_{\bar{s},\mu}$ increases the power of the log-function by one if t is even and decreases it by one if t is odd. Its reversed operator $O_{\mu,\bar{s}}$ increases the power when r is odd and decreases it when r is even.

This observation we extrapolate to speculate, in a heuristic manner, about further structural details beyond those given in Eq. (44). Sets $\mu^{-4}\log\mu$ and μ^{-4} produce only rational sets s^{-t} (if we disregard $t \geq 5$). There is thus no obvious reason to expect these sets in the general term of $C_{2\mu}$. Rather, if we accept the scheme Eq. (35a) up to $O(s^{-4})$, then (again because the matrix C_{ν}^{μ} is a full matrix) these two sets are the first sets for which there is no detailed general condition for their amplitudes. To this observation corresponds the (numerical) result that these two sets are the leading sets in the remainder R_{μ} of Eq. (44).

It follows that the next general term should be of the general order r=5. Note that E_κ^* produces, besides $s^{-4}\log s$, also a potential term (having the factor zero) $s^{-4}\log^3 s$. The latter spawns a term $s^{-5}\log^3 s$ via the operator S_1; to cancel this term, a term $\kappa^{-5}\log^2\kappa$ is required. This then would appear to be the fourth general term.

Whether or not this speculative result is correct, the point is clear that complications would increase rapidly. With these we are not going to involve ourselves any further. Instead we rewrite Eq. (44) somewhat for the purpose of representing numerical solutions.

A modification is that we combine the first two general terms in a manner which produces a simpler contribution to w_s:

$C_{2\kappa,E}$	$8w_{s,E}$
$\frac{1}{\kappa^2} - \frac{1}{4\kappa^3}$	$\left[10 + \gamma(2)\right] s^{-3} + 1.5\, s^{-4}\log s \ldots$
$\frac{4}{\kappa(4\kappa+1)}$	$10\, s^{-3} + 1.5\, s^{-4}\log s \ldots$

The difference between the two forms of $C_{2\kappa,E}$ is $O(\kappa^{-4})$ and is thus not of concern in the general term (it does of course affect R_κ).

From the remainder R_κ we split off its two leading terms. Thus

$$- C_{2\kappa} = \left[\frac{4}{\kappa(4\kappa+1)} - \frac{3\log^2\kappa}{16\pi^2\kappa^4}\right]\frac{C_\ell(1)}{4\pi} + \frac{1}{\kappa^4}\left[b_4 L_\kappa + c_4\right] + \bar{\bar{R}}_\kappa \qquad (47)$$

To represent a given numerical solution, we have to list the three constants $C_\ell(1)$, b_4 and c_4 plus the final remainder $\bar{\bar{R}}_\kappa$. We will find that the latter converges very rapidly.

VIII. THE OUTER PROBLEM

Even though Eq. (47) gives more details of the structure of the general term than Eq. (5), it would still be difficult to extract its amplitude $C_{\ell}(1)$ from a given (and necessarily truncated) numerical set $C_{2\lambda}$. The use of Eq. (15) and thus of the set $C_{2\lambda+1}$ appears preferable.

We mentioned already above at the end of Section II that for a given wing one has to determine $C_{\ell}(1)$ only for the reference downwash $w_0(y) = 1$. In Ref. 1 the extrapolation formula (1.52) was used for this purpose and led to the approximate amplitude

$$C_{\ell}(1) \approx 1.5931 \tag{48}$$

We show in this section how this value can be improved by utilizing our newly derived knowledge about the structure of the set $C_{2\lambda+1}$.

Write Eq. (15) in the form

$$C_{\ell}(1) = S(N) + \Delta(N) = 4\sum_{0}^{N}(2\lambda+1)C_{2\lambda+1} + 4\sum_{N+1}^{\infty}(2\lambda+1)C_{2\lambda+1}$$

For a given (truncated) numerical set $C_{2\lambda+1}$, the sum $S(N)$ is readily calculated. To explore the structure of $\Delta(N)$, write

$$(2\lambda+1)C_{2\lambda+1} = \frac{D_0\log\lambda + D_1}{(2\lambda+1)^2} + \frac{D_2\log\lambda + D_3}{(2\lambda+1)^3} + \ldots \tag{49}$$

in agreement with our earlier results. Using Eq. (B2), then

$$\Delta(N) = \left[(1 + \log N)D_0 + D_1\right]\frac{4N}{(2N+1)^2} + \ldots$$

This shows that the curve $S(N)$, plotted over $u = (1/N)$, has a vertical tangent at $u=0$. Its extrapolation to $u=0$ (in order to obtain $C_{\ell}(1) = S(\infty)$) would be rather unreliable.

The vertical tangent is eliminated if one uses the method of Ref. 1, writing

$$C_{\ell}(1) = S^*(N) + \Delta^*(N) \tag{50}$$

with

$$S^*(N) = S(N) + 4N(2N+1)C_{2N+1} \tag{50a}$$

Then

$$\Delta^*(N) = \frac{4N+3}{(2N+1)^2} D_0 - \left[(\log N - \tfrac{1}{2})D_2 + D_3\right] \frac{2N}{(2N+1)^3} + \ldots \tag{50b}$$

The curve $\Delta^*(N)$ has the form $O(u)$, and the curve $S^*(N)$ therefore has the form $C_\ell(1) - O(u)$. Extrapolation has now become much more reliable.

To improve the procedure of Ref. 1, we make use of the fact that the constants D_0 and D_2 in Eq. (49) are directly related to the unknown $C_\ell(1)$:

$$D_0 = C_\ell(1)/\pi^2 \quad ; \quad D_2 = -3C_\ell(1)/4\pi^2 \tag{51}$$

from Eqs. (33),(37) and (4) for D_0, Eqs. (43), (44) for D_2. In other words, we match our extrapolation procedure to the known structure of the set $C_{2\lambda+1}$. (The constants D_1 and D_3 are related to the remainder R_λ rather than to the general term and are hence unknowns; note, however, that D_1 does not appear in the leading terms of Eq. (50b).)

Inserting first only D_0, we write

$$C_\ell(1) = S^*(N) \Big/ \left[1 - \frac{4N+3}{\pi^2(2N+1)^2}\right] + \frac{a \log N - b}{(2N+1)^2} + \ldots \tag{52}$$

We can plot the first term on the right, $S^*/[\,]$, and know that its curve, extrapolated to u=0, has to have a horizontal tangent at its end point $C_\ell(1)$.

The steps which we discussed so far are illustrated in Fig. 5. The almost vertical line S* at the left is the interpolation curve of Ref. 1. There are two curved marked $S^*/[\,]$; these illustrate the remarkable increase in reliability and accuracy that is achieved by inserting the relation between $C_\ell(1)$ and D_0. The lower of the two curves is constructed using the values $C^N_{2\lambda+1}$, the results of solving the reversed system Eq. (19), truncated at $\lambda = N$. The curve through the points which have thus been calculated for a number of values N must reach $C_\ell(1)$ at u=0, but we do not know its shape near its end point.

To obtain the final (upper) curve, the values $C^N_{2\lambda+1}$ were extrapolated to $N = \infty$ for each λ. Through a remarkable coincidence, it was possible to

construct a curve, through the thus calculated points, using only the last written out term on the right of Eq. (52), without allowing for any additional terms, and using constant numbers a and b. This curve is shown in Fig. 5. It connects all calculated points to within drawing accuracy (no points were calculated beyond N = 40) even though the vertical scale of Fig. 5 is highly stretched. The first noticeable deviation between points and curve occurs to the right outside Fig. 5, at N = 10.

The end value of the new curve is $C_{\mathcal{L}}(1) \simeq 1.5930904$. It confirms the result, Eq. (48), of the less sophisticated extrapolation of Ref. 1. However, it is clear that the new value cannot be quite accurate. One, we cannot expect that the higher terms in Eq. (52) are entirely negligible; two, the number a in Eq. (52) should be related to the end result $C_{\mathcal{L}}(1)$ via Eq. (51). Making use of point two and allowing for point one we found $C_{\mathcal{L}}(1) \simeq 1.5930884$. The smallness of the difference between the two new values indicates the order of accuracy which one achieves with this extrapolative method. The last decimal of the last value is to be considered uncertain.

In the tabulation of the planar solution, Table I, we will use the amplitude number

$$a_2 = 0.1267740 \qquad \text{(Table I)} \tag{53}$$

From it follows $C_{\mathcal{L}}(1) = 4\pi a_2 = 1.5930890\ldots$. This number a_2 is treated in Table I as an exact number. It allows to construct $C_{2\mathcal{M}}$ to 8 decimals even though a_2 itself is given only to 7 decimals. To this point we will return later.

IX. THE PLANAR SOLUTION

In the last section we used the truncated set $C^N_{2\Lambda+1}$ which was obtained by solving the truncated linear system Eq. (19). The corresponding set $C^N_{2\mathcal{M}}$ is calculated by means of Eq. (13). Again the final solution $C_{2\mathcal{M}}$ has to be obtained by extrapolation. However, convergence as $N \to \infty$ is considerably slower in the case of $C^N_{2\mathcal{M}}$ than in the case of $C^N_{2\Lambda+1}$, and the required extrapolative procedure deserves a brief description.

Two successive results, $C^{N-1}_{2\mathcal{M}}$ and $C^N_{2\mathcal{M}}$, differ because of two independent reasons. One, corresponding elements $C^{N-1}_{2\Lambda+1}$ and $C^N_{2\Lambda+1}$ differ. Two, the new term C^N_{2N+1} is added in Eq. (13) when $C^N_{2\mathcal{M}}$ is calculated. The second cause has by far the larger effect. Taking this into account, we write for N large on the basis of Eq. (13)Ø

Ø A factor ½ has to be added when $\mathcal{M} = 0$. However, the extrapolative procedure is the same for all $\mathcal{M}$.

$$-C^N_{2\nu} + C^{N-1}_{2\nu} \equiv \Delta^N_\nu = \frac{1}{\pi} \frac{2NC^N_{2N+1}}{N^2 - \nu^2} (1 - \epsilon) \qquad (54)$$

The number ϵ is introduced here to cater for the first effect. Numerical testing shows that ϵ is small compared with 1.

To simplify further, we replaced C^N_{2N+1} in Eq. (54) by C_{2N+1} from Eq. (49) with the higher constants D_2, D_3, ... all set equal to zero. Using this simplified form, we calculated ϵ for N = 37,38,39,40. We found that ϵ changed little with ν, and changed even less with N.

If one assumes that ϵ is sufficiently independent of N, one can, using Eq. (B2), sum for each ν the Δ^N_ν to N=∞ and obtain a tentative final solution $C_{2\nu}$. To check the result, we repeated the procedure using N = 60. Since, within our accuracy requirement, the result was the same, we accepted it as the final result.

We calculated the Δ to 12 decimals. About 2 decimals are lost in the summation. The further calculation was done carrying 10 decimals. The final result, $\bar{\bar{R}}_\nu$, is tabulated to 8 decimals in Table I.

In Table I, the planar solution, presented in the form of Eq. (47), is denoted by $C_{2\nu,0}$ to distinguish it from the other solutions, Tables II to IV. The set $C_{2\nu,0}$ is tabulated to $\nu = 15$, and the remainder R_ν (which is $C_{2\nu,0}$ plus the general part) is tabulated in the second column.∅

To split off the leading terms of R_ν, see Eq. (47), one proceeds as follows. One chooses a tentative pivot point $\nu = p$. The amplitudes b_4 and c_4 are determined from the two conditions

$$a)\ \bar{\bar{R}}_p = 0 \ ; \qquad b)\ \sum_0^p \bar{\bar{R}}_\nu = 0 \qquad (55)$$

Condition b) arises from Eq. (2) due to the fact that all the sets in the general part as well as the two leading sets of R_ν fulfill Eq. (2) individually.

Of course, the goal is that $\bar{\bar{R}}_\nu = 0$ for all $\nu \geq p$. If p was chosen too small, then this will not be the case. The tail sum of $\bar{\bar{R}}_\nu$ will still be zero, but the values $\bar{\bar{R}}_\nu$ beyond $\nu = p$ will describe a wavy curve around the zero line. On the other hand, if p was chosen unnecessarily large, significant decimals will have been lost, and the constants b_4 and c_4 will be ill-defined.

In Table I, $\bar{\bar{R}}_\nu < 0.5\times10^{-8}$ already when $\nu = 15$. Thus knowledge of the structure of $C_{2\nu}$, Eq. (47), has enabled us to represent the slowly converging set $C_{2\nu}$ in a relatively very brief table to very high accuracy.

∅ The leading constants $C_{0,E}$ of the here required sets $C_{2\nu,E}$ are given in Appendix C.

Table I can be used to reconstruct $C_{2\mu}$ to about the accuracy of $\bar{\bar{R}}_\mu$, that is, to about 8 decimals. In doing this, one has to treat the constants a_2, b_4 and c_4 as exact numbers, even though these constants are given to 7 decimals only and are only approximations of their mathematically defined counterparts.

The inaccuracy just mentioned, the differences between the listed constants and their mathematically defined values, interferes, to the accuracy of Table I, neither with the validity of Eq. (2) nor with the manner in which $\bar{\bar{R}}_\mu$ does converge. Namely, these inaccuracies affect columns 2 and 3 only as far as the first few values (for $\mu = 0,1,2..$) are concerned, and the sum of these values is zero, for each column, closely enough to cancel out the discrepancies.

The first few values $\bar{\bar{R}}_\mu$ in Table I are not claimed to represent their mathematically exact images accurately to 8 decimals, but they are accurate to 8 decimals if the purpose is to reconstruct $C_{2\mu}$. (At the higher values of μ, of course, the inaccuracies in question affect only decimals beyond those listed.)

In the process of calculating the set $C_{2\mu}$, including C_0, no explicit use was made of Eq. (2). The fact that it was possible to extract afterwards a smoothly converging set $\bar{\bar{R}}_\mu$ which satisfies Eq. (2) serves as an overall confirmation of the numerical procedure.

It might seem contradictory that, while it is relatively easy to determine the set $C_{2\mu}$ to very high accuracy, it is considerably more difficult to determine $C_\ell(1)$. The point, already mentioned, is that $C_{2\mu}$ defines the span loading $C_\ell(y)$ well enough over the inner part of the wing but not near the wing tip. An illustration of the tip region is Fig. 6. Curves $C_\ell(y)$ are shown which have been calculated with Eq. (9a) truncated at $N = 20,25,30,35,40$. All these curves turn to $+\infty$ as $y \to 1$, where correctly, from Eqs. (5) and (A4), (see (1.47a))

$$C_\ell(y) = \left[1 + \frac{1}{16}(1-y^2)^{\frac{1}{2}} \log \frac{4}{1-y^2} \ldots\right] C_\ell(1) \cdots \tag{56}$$

To obtain the curve $C_\ell(y)$, one has to fair the curve Eq. (56) into the curve for N=40, say, at about y=0.98. The result is shown in Fig. A3.

Note that the key which makes this matching process possible lies in the fact that certain analytical functions, Eq. (A2), have Legendre coefficients which behave asymptotically like the rational sets μ^{-r}.

X. ADDITIONAL SOLUTIONS

The principle which allows to calculate additional solutions quickly once a reference solution has been determined was already indicated in Eqs. (6) and (7). We have used this principle to calculate the three solutions $C_{2\mu,i}$ for the downwash distributions

$$w_i(y) = \bar{P}_{2i}(y) \qquad (i = 1,2,3) \tag{57}$$

Together with the reference planar solution $C_{2\mu,0}$, these solutions form a set of four independent solutions (and thus represent, by linear superposition, a three-fold multitude of solutions).

The sets $C^N_{2\mu,i}$ were calculated for N = 60. By comparing the tail of a set $C^N_{2\mu,i}$ with that of $C^N_{2\mu,0}$, a preliminary value X was obtained and, using this value, a preliminary void set $C^N_{2\mu,iv}$ was calculated. Since for this set the constant D_0 in $C_{2\lambda+1}$ is (almost) zero by definition, extrapolation to N=∞ is simplified. The resulting set is treated essentially like the set R_μ in the reference case, except that now there is, in addition to b_4 and c_4, a third parameter, namely, a small adjustment ΔX to X. This parameter is necessary to make the final remainder $\bar{R}_\mu$ converge towards zero without waviness. In this numerical step, we again carried 10 decimals. No difficulty was encountered when p = 25 was chosen as the pivot point. The results, again rounded to 8 decimals, are listed in Tables II to IV.

A graphical presentation of the four solutions $C_{\ell,i}$ and their respective downwash distributions w_i is Fig. 7. All curves $C_{\ell,i}$ form a downwash hook near the tip with a vertical tangent at the tip itself; however, in the presentation of Fig. 7 this hook is too small to be recognizable when i=3 or i=4. The corresponding void curves $C_{\ell,iv}$ are shown in Fig. 8.

The relative scales of $C_{\ell,i}$ and w_i are chosen in Fig. 7 such that $C_{\ell,0}$ and w_0 have about the same amplitude. For i≠0, the amplitudes of the waves in $C_{\ell,i}$ are much smaller than the amplitudes of the corresponding waves in w_i. The amplitude ratios correspond roughly to the ratio between half-wave length and wing span (this is what one would expect from slender wing theory).

An interesting observation is the following: one may form the ratio between two integrals over the wing area, the lift integral and the downwash momentum integral. For a planar wing this ratio is $\frac{1}{2}C_L$. For the void parts of the solutions i = 1, 2 and 3, this ratio is found to differ from that for the planar wing by less than 1%. As one calculates the same ratio for the complete solutions, Fig. 7, small differences between large figures have to be formed, and the resulting ratio varies somewhat more, between 0.895 for i=0 and 0.821 for i=3. The indication remains that, as far as the total lift of a given wing is concerned, the details of how the total downwash is

distributed over the wing span are of relatively little relevance. The details of this distribution tend to have negligible effect on the outer flow.

We have discussed in this section only the span loading functions $C_{\ell_i}(y)$. The complete pressure distributions $p(\xi,y)$ of closely related solutions are discussed in Appendix D. These provide further interesting insight into the mechanism of lifting surfaces.

XI. GENERALIZATION OF THE SOLUTION

Pressure singularities of orders $-\frac{1}{2}$ (l.e.) and $+\frac{1}{2}$ (t.e.) arise due to linearization at those wing edges which cross the direction of the undisturbed flow. These singularities are well understood. The wing tip problem is the problem of the transition, between the two types of singularities, where the wing edge becomes parallel to the flow. This problem is considerably more involved. We were able to resolve it for the specific case of the circular wing because here a complete set of analytical relations of relative simplicity are available: the elementary pressure solutions in Eq. (9); the reversible relation between the two sets of coefficients, those for the span loading and those for the chordwise moments, Eqs. (13) & (14); the relation between amplitude coefficients and downwash coefficients, Eq. (18).

Corresponding analytical tools are not available for wings of arbitrary planform, and it will not readily be possible to determine the details of the solutions for such wings to the extent that we did in Eq. (47) for the circular wing. On the other hand, it is in the nature of the lifting surface mechanism that the type of pressure singularity which arises at a local wing singularity is not affected by the far field from other parts of the wing. For the circular wing, we found that the leading part of the pressure singularity is independent even of the slope of the downwash distribution at the tip and is determined solely by the geometric tip shape; the remainder part which describes a particular solution goes to zero and does so of higher order as the tip is approached. The essence of this observation must be valid for all wings having parabolic wing tips, and the reference length for the coordinates which describe the tip singularity must be the wing tip radius R_T.

Since to bring this qualitative statement into a detailed quantitative form would require extensive further investigations, we confine our present observations to a few main points. In particular, we do not concern ourselves with details of the pressure distribution (which we did not discuss, beyond Fig. 2 and Appendix D, even for the circular wing). The span loading distribution is more readily discussed since here we have available certain analytical functions which conveniently describe the leading terms of the limit behavior at the tip.

The analytical functions in question are those whose sets $F^r_{2\nu}$ of Legendre coefficients converge like the rational sets E_ν, see Eqs. (A2,2a). Hence we can represent the first two general sets of Eq. (44) as already shown in Eq. (56) where, on the right, we should add a remainder function R(y). However, we do not have a corresponding analytical function for the set $\nu^{-4}\log^2\nu$. A further difficulty, discussed in Appendix A, is that already a set $O(\nu^{-4})$ might have a finite tangent at the tip, Fig. A1, or a vertical tangent, Fig. A2. To decide on this point one has to review the complete set, not only its rate of tail convergence[Ø]. To avoid further discussion of such higher order details we confine our further attention to the two terms already given in Eq. (56).

Let b be the wing span, so that $u = (1-y)b/2R_T$ is the proper spanwise coordinate for describing the wing tip singularity asymptotically near the tip $y=+1$. Here $(1-y^2)\approx 2u$ for the circular wing. For general wing planforms, we can hence write the local lift $\ell(y)$ as

$$\ell(y) = \left\{\left[1 + \frac{1}{16}\left((1-y^2)b/2R_T\right)^{\frac{1}{2}}\log\frac{8R_T}{(1-y^2)b}\right] C_\ell(1) + R(y)\right\} c(y)q \qquad (58)$$

We use the wing chord c(y) since the curve $\ell(y)$ tends, to a degree, to imitate c(y) over the inner part of the wing. Considering two wings having the same tip radius, the difference between the two chords is O(uc(y)) near the tip and is hence of higher order.

The complete lift function $\ell(y)$ has a vertical tangent, but it differs from the parabolic type $O(u^{\frac{1}{2}})$ of c(y) by the log-term. The remainder function R(y) of Eq. (58), taken by itself, may be expected to go to zero about like $O(u^{\frac{1}{2}})$.

The generalized form of the solution, Eq. (58), is valid for any aspect ratio and thus in particular for the slender wing. For the elliptic wing, slender wing theory predicts an elliptic span loading, that is, Eq. (58) without the log-term and without R(y). The log-term is of the order $u(AR)^{\frac{1}{2}}\log u$ if AR the aspect ratio. It follows, as a sample application of Eq. (58), that slender wing theory is valid strictly only in the limit $AR\to 0$.

Ø The void span loading curves Fig. 8 represent void functions R(y) and appear to have finite tangents. However, it might be that the small component $O(\nu^{-4}\log\nu)$ in R_ν enforces a vertical tangent; this detail would not be visible in the scale of Fig. 8.

XII. CONCLUSIONS

In the earlier paper[1] we had shown that the apparent divergence of the Kinner[3] series is eliminated by the physically necessary condition that the infinite set of span loading coefficients $C_{2\kappa}$ has a zero sum, and that the properties of the sum of the Kinner series can be investigated by means of the sets of Legendre coefficients of certain analytical functions. We had further shown that, in order to have a finite downwash inside the tip, the span loading function must have a logarithmic component.

This earlier analysis is pursued further in the present paper and is brought to its logical conclusion. The duality between the set $C_{2\kappa}$ and the set $C_{2\lambda+1}$ of moment coefficients is worked out, and the close relationship between the $C_{2\lambda+1}$ and the downwash coefficients w_s is formulated and is utilized.

It is shown that either C-set has to contain logarithmic elementary sets in addition to rational sets, and the asymptotic description of the pressure singularity at the wing tip is constructed. Its elementary sets are identified up to the order of the "void" part of the solution, the latter being that part of a specific solution which distinguishes it from a reference solution. The void part converges to zero at the tip, essentially like $u^{3/2}$ if u is the distance from the tip referred to the tip planform radius R_T.

With the structure of the solutions thus identified, it becomes relatively easy to calculate numerical solutions to very high accuracy, in particular once a reference solution has been determined. Furthermore, only a short tabulation is required to fully describe such a solution.

The main analysis of this paper deals specifically with the circular wing in incompressible flow. The form of the general solution for arbitrary wings with parabolic wing tips is briefly discussed. This form shows in particular that the result of slender wing theory is valid strictly only in the limit of zero aspect ratio.

Certain conclusions of direct engineering interest can be drawn from the calculated sample solutions for the circular wing. One, the details of how the total given downwash is distributed over the wing span affects the total lift relatively little. Two, a spanwise wavy incidence distribution is well reproduced by corresponding waves in the pressure distribution along the wing leading edge, but over the rear part of the wing no visible waviness in the pressure remains (assuming, of course, that the wavelength is relatively short).

A by-product of the analysis are two sets of formulas of general mathematical interest. These formulas connect the sums of infinite progressions involving the ψ-function (and thus the logarithm) to the Riemann ζ-function and seem to be the first formulas of this kind.

REFERENCES

1. P. F. Jordan: The Parabolic Wing Tip in Subsonic Flow. AIAA Paper # 71-10 (New York, Jan. 71). Also, AFOSR-TR-71-0075.

2. P. F. Jordan: Span Loading and Wake Formation. Aircraft Wake Turbulence and its Detection, Plenum Press 1971, pp. 207-227. Also, AFOSR 70-2873 TR.

3. W. Kinner: Die kreisförmige Tragfläche auf potentialtheoretischer Grundlage. Ing. Archiv 8 (1937) pp. 47-80.

4. Handbook of Mathematical Functions; National Bureau of Standards (3rd printing 1965). M. Abramowitz and I. A. Stegun, editors.

$\mathcal{N}$	$C_{2\mathcal{N},0}$	$C_{2\mathcal{N},0} + [\cdot]a_2$	$\bar{\bar{R}}_{\mathcal{N}}$
0	+.22375288	+.04654659	+.00184543
1	-.14455778	-.04313858	-.00148142
2	-.03065010	-.00255042	-.00030011
3	- 1349032	-. 52375	- 4664
4	- 761010	-. 17088	- 1125
5	- 489108	-. 7158	- 355
6	- 340778	-. 3510	- 134
7	- 251341	-. 1919	- 57
8	- 192964	-. 1137	- 27
9	- 152820	-. 716	- 13
10	- 124027	-. 473	- 7
11	- 102674	-. 325	- 4
12	- 86400	-. 231	- 2
13	- 73712	-. 168	- 1
14	- 63628	-. 125	- 1
15	- 55481	-. 96	($\mathcal{N}\geq 15$) 0

$$C_{2\mathcal{N},0} + \left[\frac{4}{\mathcal{N}(4\mathcal{N}+1)} - \frac{3\ \log^2\mathcal{N}}{16\pi^2\mathcal{N}^4}\right] a_2 + \frac{1}{\mathcal{N}^4}(b_4 L_{\mathcal{N}} + c_4) + \bar{\bar{R}}_{\mathcal{N}} = 0$$

$$a_2 = 0.1267740$$
$$b_4 = 0.0029655$$
$$c_4 = 0.0416545$$

$$w_0(y) \equiv 1$$

Table I. Planar Solution $C_{2\mathcal{N},0}$

$\mathcal{N}$	$C_{2\mathcal{N},1v}$	$\bar{\bar{R}}_{\mathcal{N}}$
0	-.08355512	+.20721931
1	+.10240765	-.21639945
2	-.01601144	+.00870664
3	-.00186437	+. 40008
4	-. 52361	+. 5546
5	-. 20553	+. 1224
6	-. 9737	+. 355
7	-. 5216	+. 124
8	-. 3048	+. 49
9	-. 1902	+. 22
10	-. 1248	+. 10
11	-. 854	+. 5
12	-. 604	+. 3
13	-. 439	+. 2
14	-. 327	+. 1
15	-. 249	+. 1
16	-. 192	($\mathcal{N}\geq 16$) 0

$$C_{2\mathcal{N},1v} + \frac{1}{\mathcal{N}^4}(b_4 L_{\mathcal{N}} + c_4) + \bar{\bar{R}}_{\mathcal{N}} = 0$$

$$a_2 = 0$$
$$b_4 = 0.0086548$$
$$c_4 = 0.1053370$$

$$w_{1,v}(y) = \bar{P}_2(y) - X = (5y^2 - 1)/4 - 0.4324159$$

Table II. Solution $C_{2\mathcal{N},1v}$

μ	$C_{2\mu,2v}$	$\bar{\bar{R}}_\mu$
0	-.05930407	+.30776604
1	+.04670161	-.27618971
2	+.02349934	-.03789344
3	-.00856274	+.00571340
4	-. 137425	+ 47133
5	-. 46234	+ 9207
6	-. 20422	+ 2548
7	-. 10521	+ 865
8	-. 6001	+ 337
9	-. 3683	+ 145
10	-. 2389	+ 67
11	-. 1620	+ 33
12	-. 1138	+ 17
13	-. 823	+ 9
14	-. 610	+ 5
15	-. 462	+ 3
16	-. 357	+ 1
17	-. 280	+ 1
18	-. 222	($\mu \geq 18$) 0

$$C_{2\mu,2v} + \frac{1}{\mu^4}(b_4 L_\mu + c_4) + \bar{\bar{R}}_\mu = 0$$

$$a_2 = 0$$
$$b_4 = 0.0024522$$
$$c_4 = 0.2270359$$

$$w_{2,v}(y) = \tilde{P}_4(y) - X = (21y^4 - 14y^2 + 1)/8 - 0.2795066$$

Table III. Solution $C_{2\mu,2v}$

κ	$C_{2\kappa,3}$	$\bar{\bar{R}}_\kappa$
0	-.04502880	+.43750001
1	+.03210567	-.39520727
2	+.00938151	-. 3174875
3	+.01056414	-. 1494365
4	-.00519578	+. 381883
5	-. 98681	+. 42559
6	-. 37073	+. 10118
7	-. 17716	+. 3217
8	-. 9684	+. 1211
9	-. 5786	+. 510
10	-. 3686	+. 233
11	-. 2466	+. 113
12	-. 1716	+. 57
13	-. 1232	+. 30
14	-. 908	+. 16
15	-. 685	+. 9
16	-. 526	+. 5
17	-. 411	+. 3
18	-. 326	+. 1
19	-. 262	+. 1
20	-. 213	($\kappa \geq 20$) 0

$$C_{2\kappa,3v} + \frac{1}{\kappa^4}(b_4 L_\kappa + c_4) + \bar{\bar{R}}_\kappa = 0$$

$$a_2 = 0$$
$$b_4 = -0.0156775$$
$$c_4 = 0.3787791$$

$$w_{3,v}(y) = \bar{P}_6(y) - X$$

$$= (429y^6 - 495y^4 + 135y^2 - 5)/64 - 0.2068387$$

Table IV. Solution $C_{2\kappa,3v}$

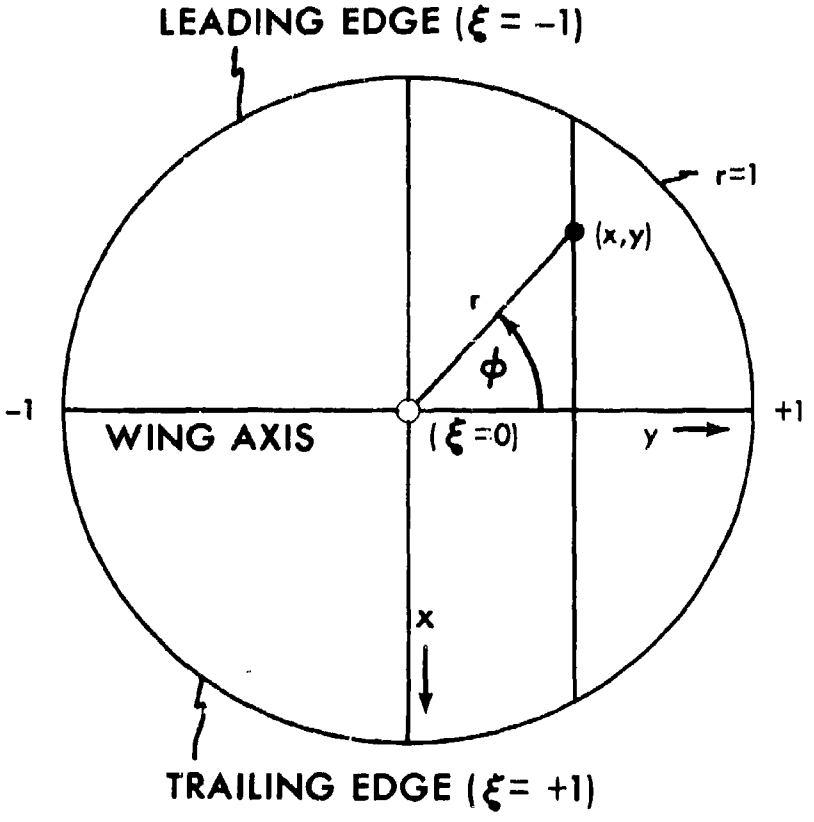

Fig. 1. Coordinates of Circular Wing

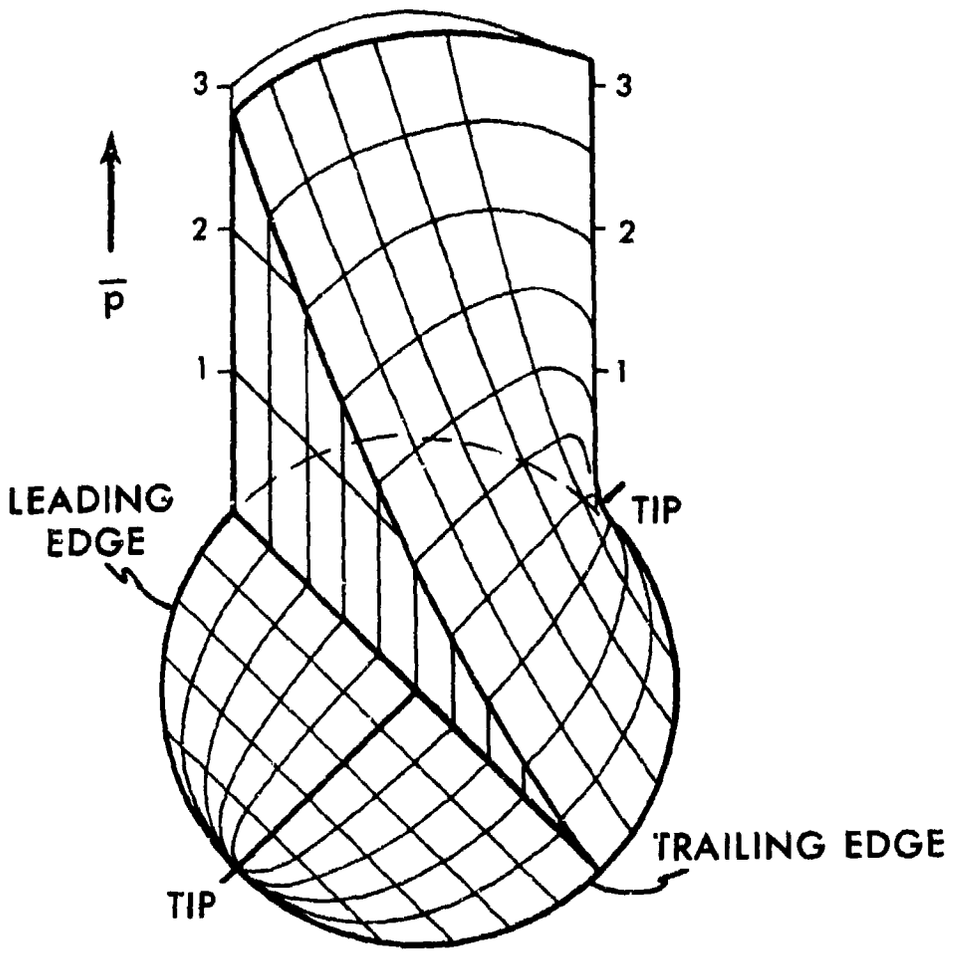

Fig. 2. Relief of Pressure Function $\bar{p}$ over Right Half of Planar Circular Wing

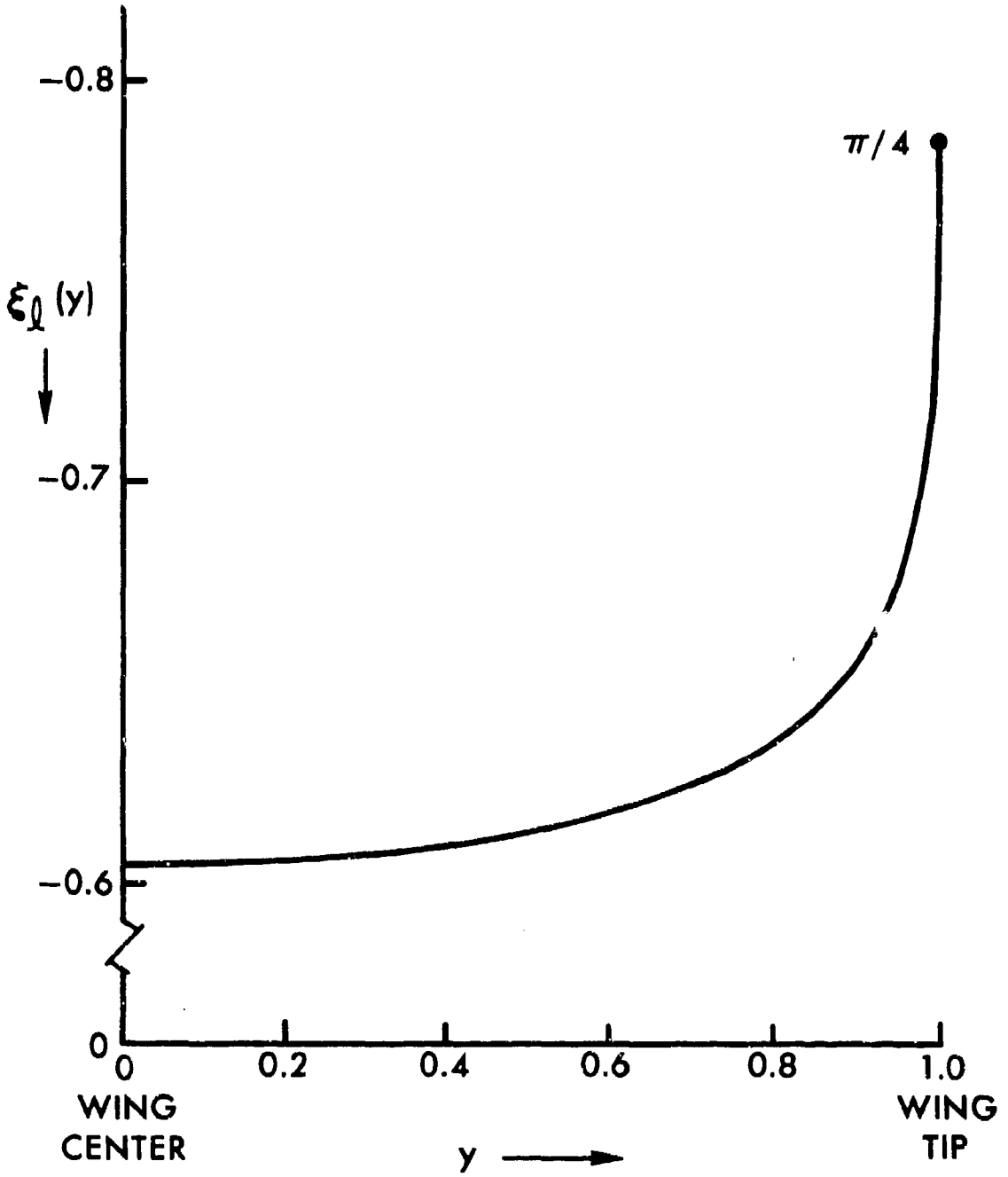

Fig. 3. Chordwise Position of Center of Pressure over Wing Span

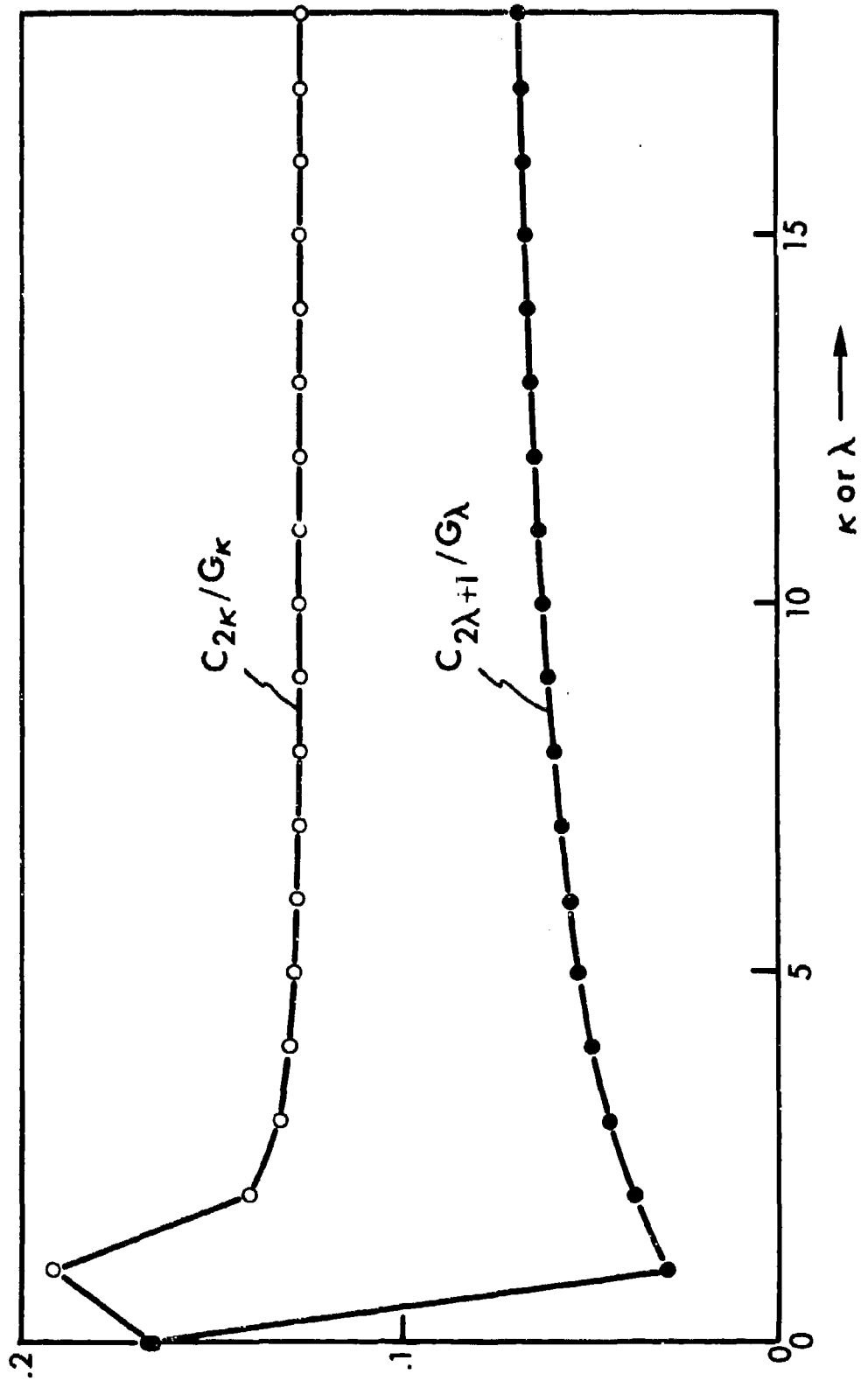

Fig. 4. Coefficients of Planar Solution (comp. Eqs. (34a,b))

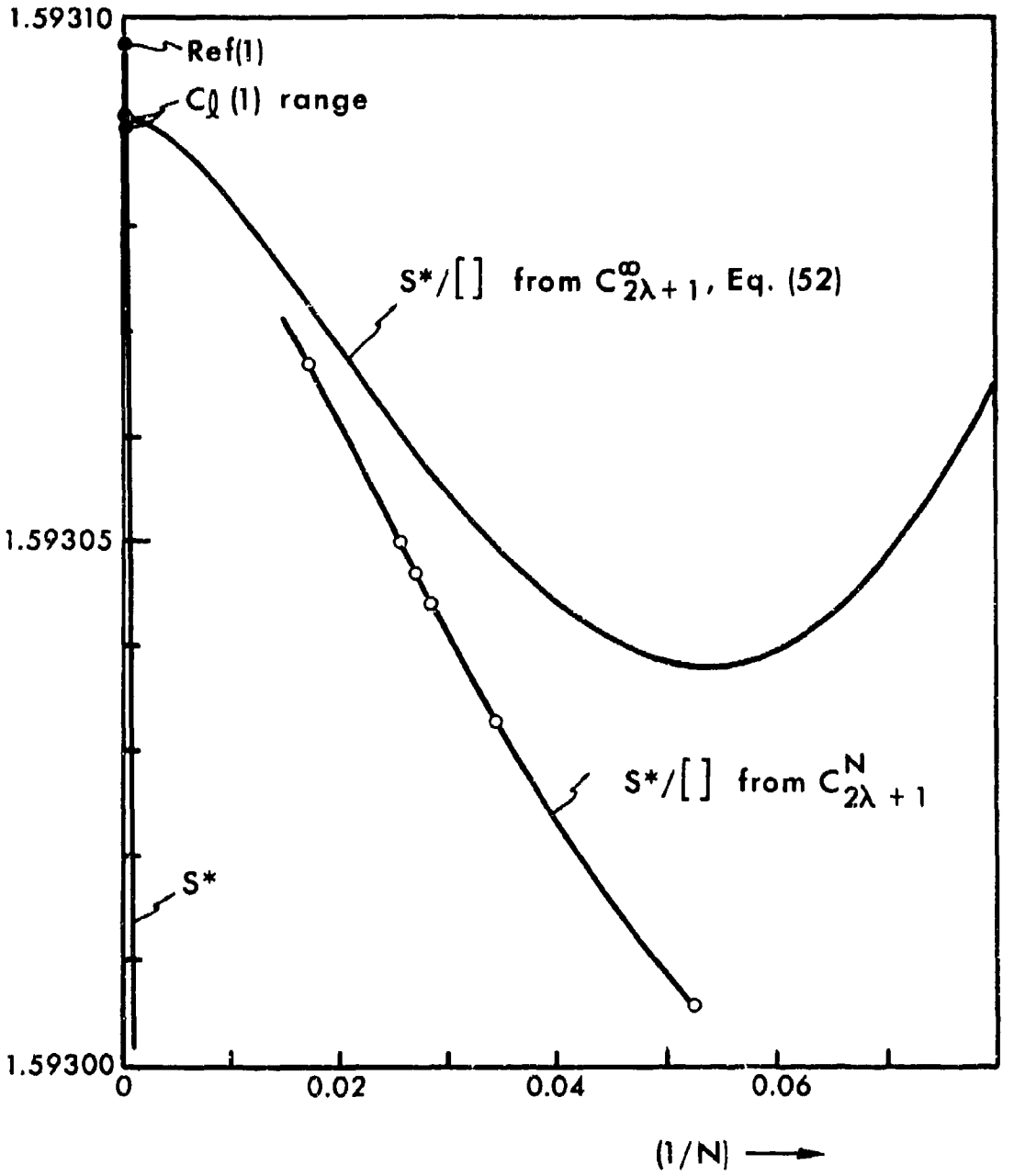

Fig. 5. Extrapolation to Determine $C_\ell(1)$

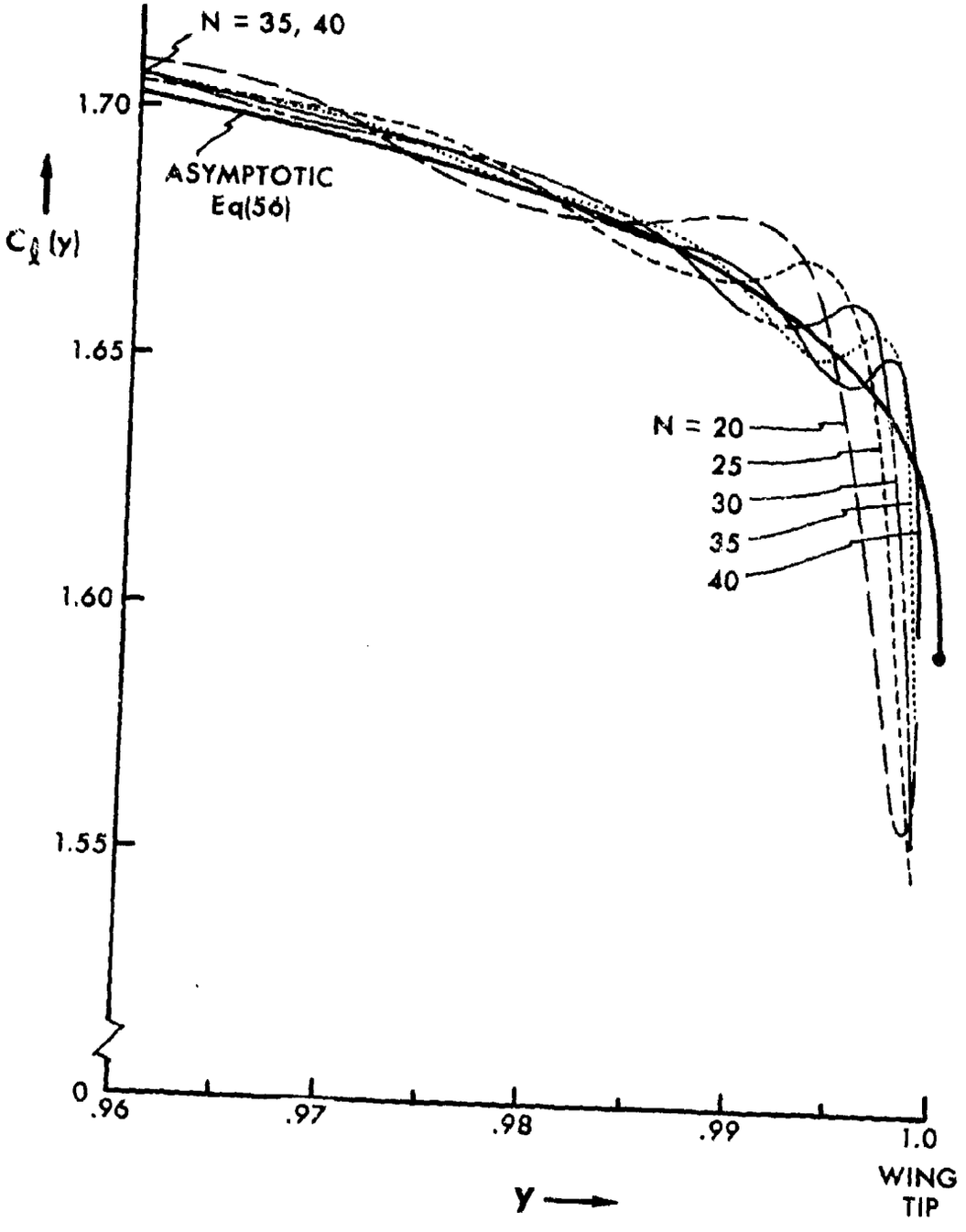

Fig. 6. Convergence of Legendre Series for Span Loading Functions near Wing Tip

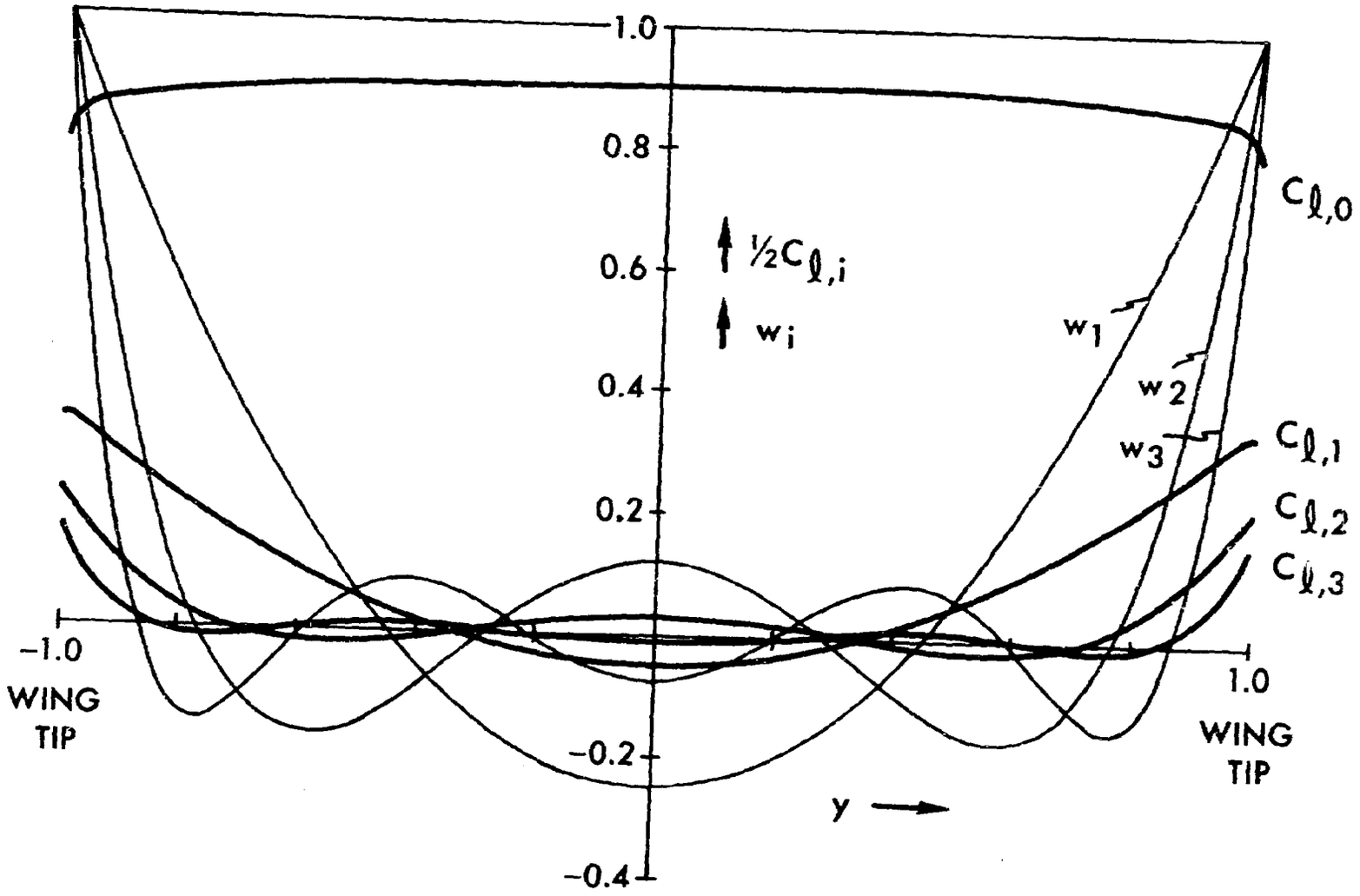

Fig. 7. Span Loadings $C_{\ell,i}$

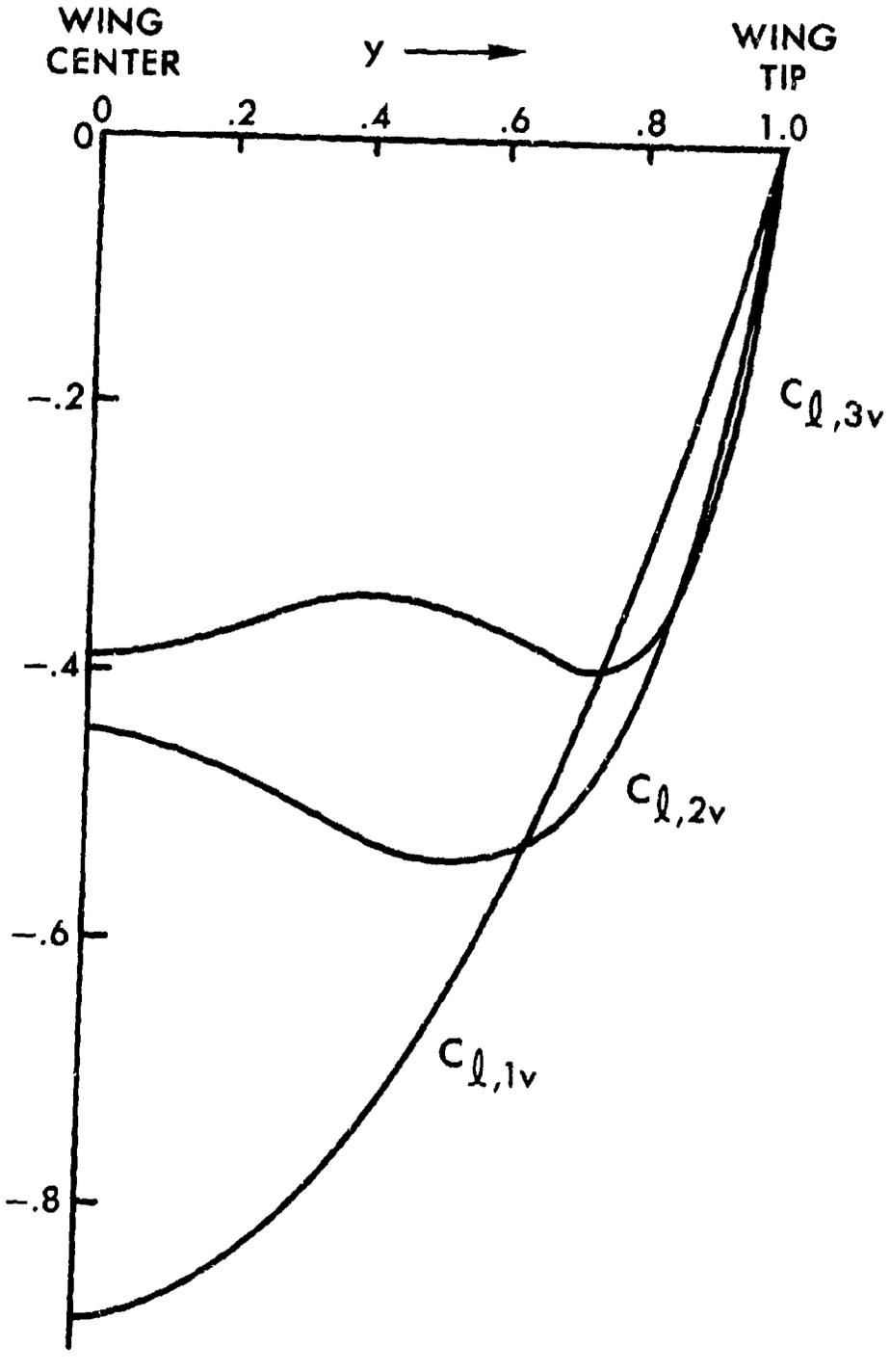

Fig. 8. Void Span Loadings $C_{\ell,iv}$

APPENDIX A

ELEMENTARY SPAN LOADING FUNCTIONS

In the analysis of this paper the solving set $C_{2\mu}$ forms an intermediary between given downwash w and required pressure distribution p. The critical analytical problem arises in the relation between w and $C_{2\mu}$, and the elementary sets E_μ which are used to build up $C_{2\mu}$ are taylored for this critical problem. Comparatively, the relation between $C_{2\mu}$ and, say, the span loading $C_\lambda(y)$ is a simple mathematical formula, Eq. (9a). Nevertheless, this formula does not give the reader an immediate illustration of the contributions of the sets E_μ to $C_\lambda(y)$. The purpose of this Appendix is to provide this illustration.

If E_μ occurs in the general term of Eq. (6), then its contribution to $C_\lambda(y)$ is

$$C_\lambda^E(y) = \frac{-1}{2(1-y^2)^{\frac{1}{2}}} \sum_0^\infty E_\mu P_{2\mu}(y) \tag{A1}$$

if the normalization $C_\lambda(1) = 1$ is made. We use Eq. (A1) as our definition of elementary span loading functions.

In Ref. 1 elementary sets $F_{2\mu}^r$ were considered whose span loading functions are simple analytical functions, see Table I of Ref. 1. Abbreviate by writing $\bar{y}$ for $(1-y^2)^{\frac{1}{2}}$; then, for $r \geq 2$,

$$2C_\lambda^E(y)_{E=F_{2\mu}^r} = \begin{cases} \bar{y}^{r-2} & \text{if r is even} \\ \bar{y}^{r-2}\log(2/\bar{y}) & \text{if r is odd} \end{cases} \tag{A2}$$

The first six of these functions are plotted in Fig. A1. In standard collocation analyses, only the functions with r=2,4,6.. are used. Of these, r=2 denotes the strictly elliptic distribution (a straight horizontal line in Fig. A1). The curve r=4 has a finite tangent at the tip; the subsequent curves r=6,8.. have zero tangents. On the other hand, the correct curve $C_\lambda(y)$ has a vertical tangent at the tip. Clearly, one has to include the function r=3 if one wants to properly represent this fact.

The curves for the sets μ^{-r}, Fig. A2, have a different tip behavior; they converge toward a finite limit curve which has a vertical tip tangent. This limit function is determined by the initial coefficients of the limit set. Namely, for $r \to \infty$

$$C_0 \to 1; \quad C_2 = -1; \quad C_{2\mu} \to 0 \text{ if } \mu \geq 2 \tag{A3}$$

The limit function in Fig. A2 is hence

$$C_{\mathcal{L}}^{E}(y) = 3(1-y^2)^{\frac{1}{2}}/4 \qquad (r \to \infty) \tag{A3a}$$

On the other hand, the tip behavior of the curves in Fig. A1 is produced by the tail behavior of the sets $F_{2\mu}^{r}$:

$$F_{2\mu}^{r} \sim \sum_{\nu \geq r}^{\infty} c_{\nu r}/\mu^{\nu} \tag{A2a}$$

We can use this fact to determine, by means of Eq. (A2), the tip behavior of the curves for μ^{-2} and μ^{-3} in Fig. A2. The result is

$$C^{E}(y)_{E=\mu^{-2}} = 1 + \tfrac{1}{2}\bar{y}\log(2/\bar{y}) + \ldots$$

$$C^{E}(y)_{E=\mu^{-3}} = \qquad \tfrac{1}{2}\bar{y}\log(2/\bar{y}) + \ldots \tag{A4}$$

see (1.33). There would be no point in pursuing this comparative procedure further. Already for r=4 it yields a leading term, $O(\bar{y}^2)$, which is overshadowed by the limit function, Eq. (A3).

Also plotted in Fig. A2 are the curves for the logarithmic sets $\mu^{-4}L_{\mu}$ and $\mu^{-4}\log^2\mu$. The former has $C_2 = -1$ and $C_0 \approx 1$. The contributions of the first two Legendre polynomials to its function $C^{E}(y)$ thus correspond to those of the sets μ^{-r}. Accordingly, its curve fits well between those for μ^{-3} and μ^{-4}. On the other hand, in the case of the set $\mu^{-4}\log^2\mu$, we have $C_2 = 0$ and C_0 small. Therefore, its curve remains close to the zero line also over the main part of the wing span.

By combining the curves for μ^{-2}, μ^{-3} and $\mu^{-4}\log^2\mu$ of Fig. A2, we can form the curve for the span loading due to the general term of Eq. (44). However, taken by itself this span loading would not be very meaningful. Of the three conditions that the terms of orders $s^{-3}\log s$, s^{-3} and $s^{-4}\log s$ in w_s must be zero, it does fulfill the first and the last but not the second. To fulfill the second condition also, we add the set μ^{-4} (other sets could be used instead, e.g. the set Eq. (A3)). We then get a refined form of the "basic solution" (1.48).

First, we reformulate the latter to conform to the modification Eq. (47). Thus

$$E_{\kappa,\text{basic}*} = \frac{4}{\kappa(4\kappa+1)} + \bar{a}_4/\kappa^4 \tag{A5}$$

The second condition is fulfilled by setting

$$\bar{a}_4 = 5/\left[\, 8\zeta(2) + 2\zeta(3)\right] = 0.3212627..$$

To fulfill also the third condition, we have to add the third general term:

$$E_{\kappa,\text{basic}**} = \frac{4}{\kappa(4\kappa+1)} - \frac{3\log^2\kappa}{16\pi^2\kappa^4} + \bar{\bar{a}}_4/\kappa^4 \tag{A6}$$

For this the second condition yields

$$\bar{\bar{a}}_4 = \frac{5 + 3\left[4\zeta_{ee}(2) + \zeta_{ee}(3)\right]/8\pi^2}{8\zeta(2) + 2\zeta(3)} = 0.3412738..$$

where

$$\zeta_{ee}(r) = \sum_1^\infty \frac{\log^2\kappa}{\kappa^r}$$

and specifically

$$\zeta_{ee}(2) = 1.989280. \quad ; \quad \zeta_{ee}(3) = 0.239747..$$

The span loading curves for these two basic sets are shown in Fig. A3. The vertical scale of this figure is stretched. Repeated for comparison is the curve r=2 from Fig. A2; this curve cuts over the basic curves near the tip (compare Fig. 4 of Ref. 1) because its log term in Eq. (A5) is too large by a factor 2 for the first of the above three conditions to be fulfilled.

Also shown in Fig. A3 is the planar solution; it also is here normalized to $C_\ell(1) = 1$. This solution approaches the basic solutions asymptotically at the tip, as, indeed, must any solution (for any downwash w(y)).

That the planar solution agrees well with the basic solutions over the inner part of the wing span also is fortuitous. In this latter respect other solutions are quite different, see Fig. 7.

To the illustrations of elementary span loadings, Figs. A1 to A3, Fig. A4 adds a few illustrations of corresponding elementary downwash distributions. Denoted by w_2 is the curve due to μ^{-2} alone; this curve does not fulfill any one of the three conditions and goes to $-\infty$ at the tip. The curve $w_2 - w_3/4$, due to $\mu^{-2} - \mu^{-3}/4$, fulfills the first condition and hence approaches the tip more smoothly than the first. For the last two curves, a third term is added to fulfill the second condition also; thus here $w(1)$ is finite (but $w'(1)$ is infinite). In one of the two curves the added set is the infinite set μ^{-4} (that is, this is the "basic solution" (1.48)); in the case of the other curve, the finite set Eq. (A3) is added. One sees that the "basic solution" approaches the case of a constant downwash reasonably well. On the other hand, the use of the set Eq. (A3) introduces a curvature corresponding to that of the limit function Eq. (A3a).

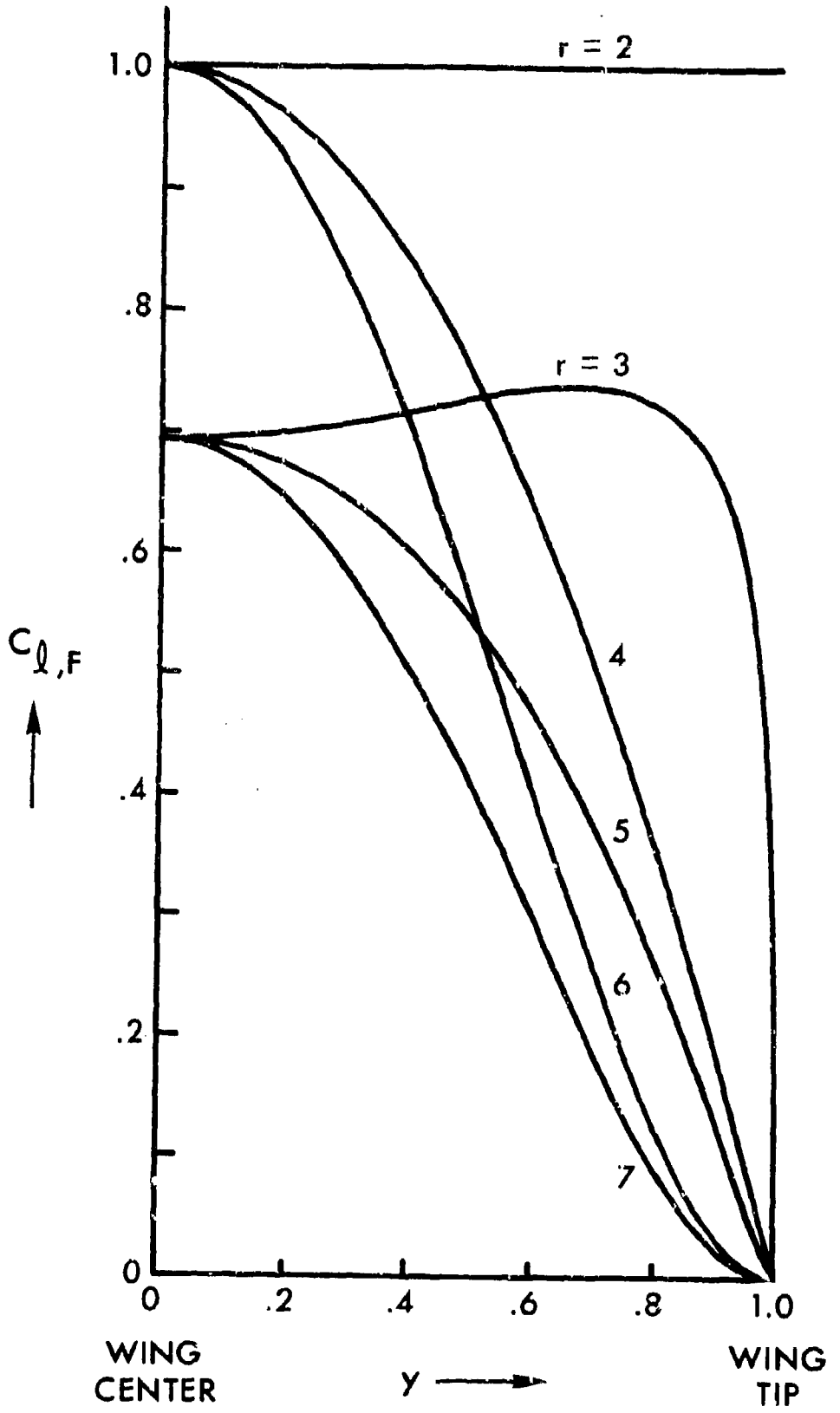

Fig. A1. Elementary Span Loading Functions $C_{\ell,F}$ due to F^{r}_{2K}

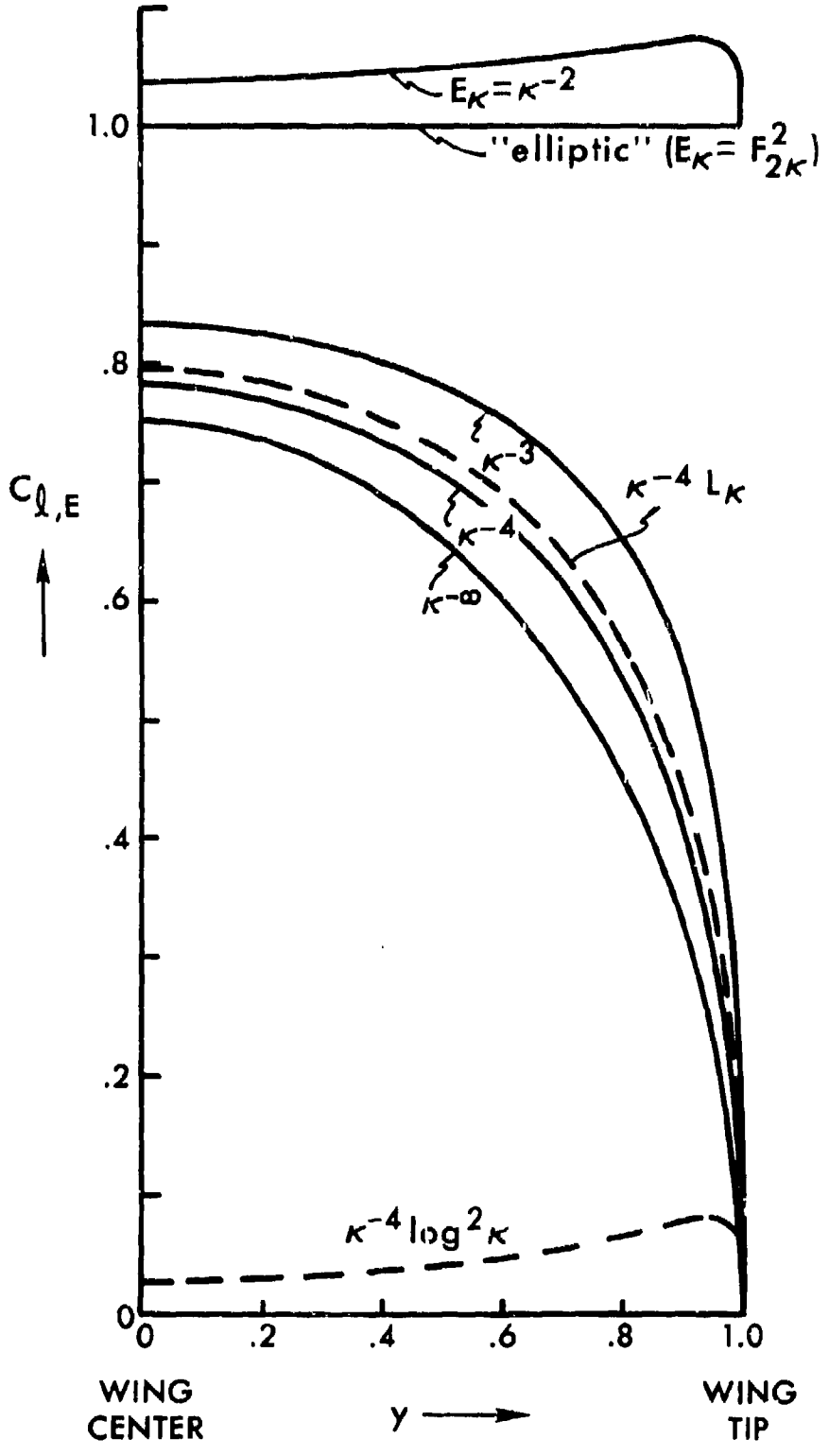

Fig. A2. Elementary Span Loading Functions $C_{\ell,E}$

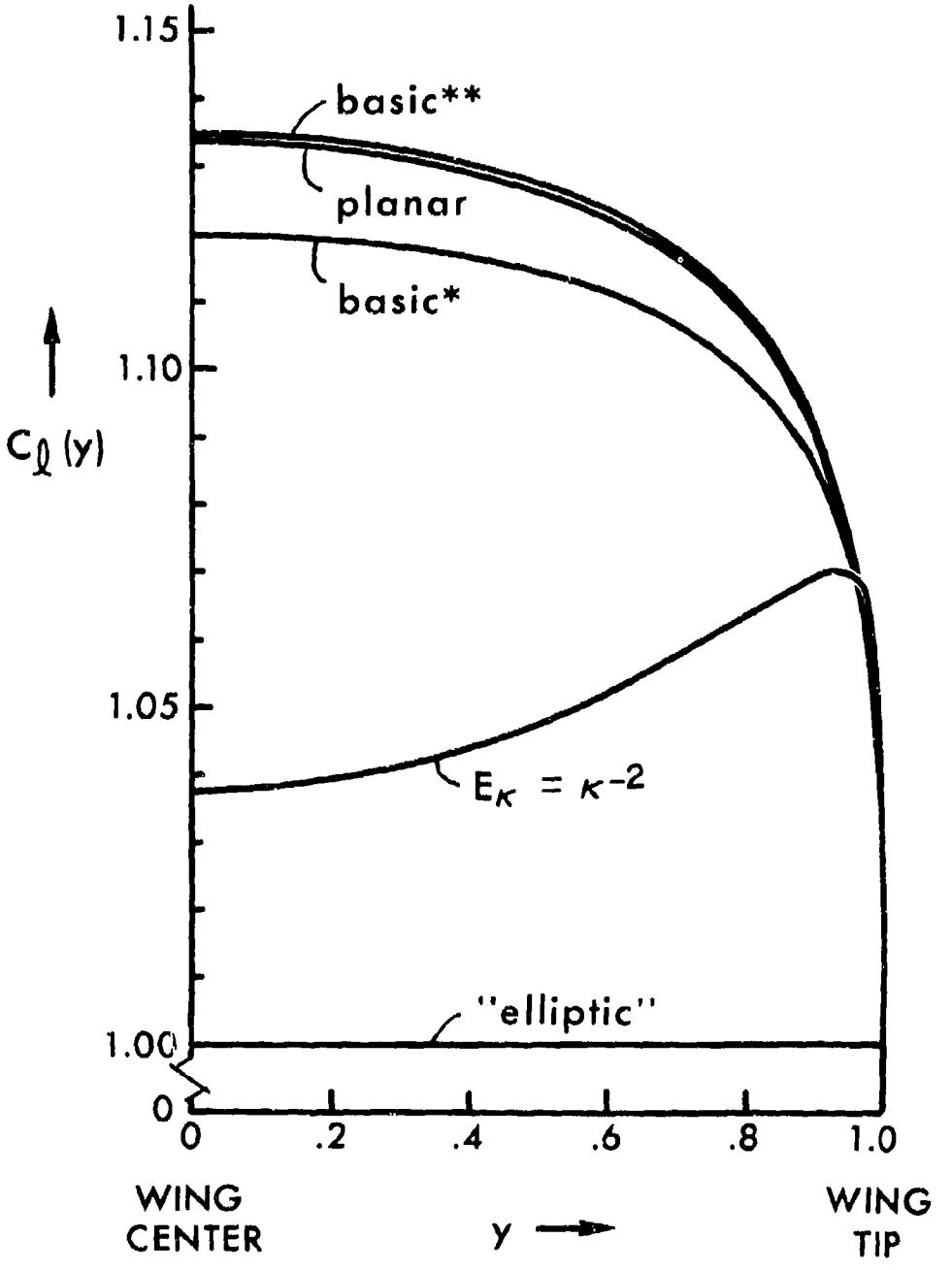

Fig. A3. Basic Span Loading Functions

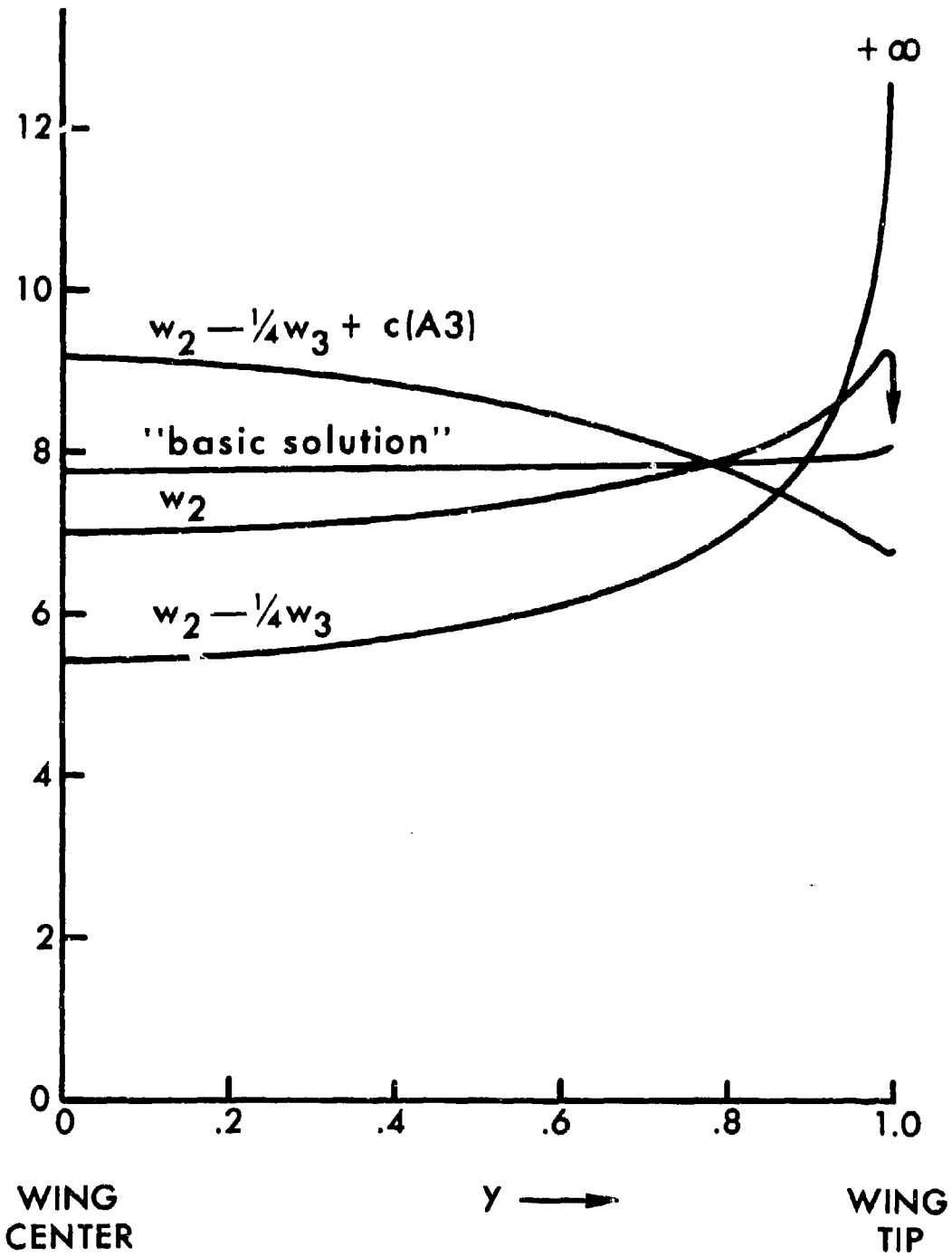

Fig. A4. Elementary Downwash Distributions

APPENDIX B

SUMMATION FORMULAS

In the analysis of this paper the sum

$$S_E = \sum_{\kappa=1}^{\infty} E_\kappa \tag{B1}$$

of an infinite set E_κ is frequently required. For example, one needs S_E to determine the leading coefficient E_0 by means of Eq. (2). Since the E_κ are progressions, term-by-term summation is not a practical proposition (the rate of convergence slows down indefinitely as the summation proceeds).

Numerical tables (e.g., of the ζ-function or the ψ-function) are sometimes available from which S_E can be read either directly or after some transformation. This is not the case, for example, if E_κ contains $\log\kappa$. Still, high numerical accuracy is obtained by means of the formula, obtained from 25.4.1 of Ref. (4)

$$\sum_{N+1}^{\infty} E_\kappa = \int_N^{\infty} E(x)dx - \frac{1}{2}E_N - \frac{1}{12}\left(\frac{dE(x)}{dx}\right)_{x=N} + \ldots \tag{B2}$$

The only requirement here is that the function $E(x)$ which interpolates E_κ can be integrated, either analytically, or numerically after transformation of the integral onto a finite range.

Because Eq. (B2) is available, there is no absolute need for the closed form summation formulas which we will derive next. These formulas are of considerable mathematical interest, however, because they appear to be the first of their kind, namely, the first to involve the logarithm.

Consider the sets $C_{2\lambda+1,E}$ which are given in Eqs. (33, 33a). From Eq. (15a) follows

$$\sum_{\lambda=0}^{\infty} \bar{\lambda}\, C_{2\lambda+1,E} = 0 \tag{B3}$$

except if r=2. Performing this summation for r even, one obtains the familiar closed form expression for $\zeta(2n)$, see 23.2.16 of Ref. (4). No corresponding expression for $\zeta(2n+1)$ seems to exist.

Performing the summation Eq. (B3) for r odd, we obtain a new kind of result. Making use of 23.2.20 of Ref. (4) and of some simple transformations, we find for r=3

$$\sum_{n=1}^{\infty} \frac{L_n}{(2n-1)^2} = \left[7\zeta(3) + 12\zeta(2)\log 2\right]/16 \qquad \text{(B4a)}$$

Correspondingly for r=5

$$\sum_{n=1}^{\infty} \frac{L_n}{(2n-1)^4} = \left[31\zeta(5) - 6\zeta(2)\zeta(3) + 60\zeta(4)\log 2\right]/64 \qquad \text{(B4b)}$$

The set L_n here is given by Eq. (31a). It contains log n and is closely related to the ζ-function.

The procedure is readily continued for r=7, 9.. . Note that the resulting formulas, Eqs. (B4), are homogeneous of order r if one counts as follows: one counts the arguments of the ζ-functions, counts the power of the denominator on the left, counts L_n as 1, and notices that log 2 = η(1), see 23.2.19 of Ref. (4).

The formulas Eqs. (B4) are related to the sets $C_{2\lambda+1,E}$ through the form of the denominator on the left. In order to obtain formulas which are related to the elements κ^{-r} of $C_{2\kappa}$, one reverses the process, setting $E_\lambda = (1/\bar{\lambda}^t)$, applies S_0^{-1} to obtain the corresponding sets $C_{2\kappa,E}$, and makes use of Eq. (2). For t odd this leads again to the familiar expression for $\zeta(2n)$. For t=4 and t=6 one finds

$$\sum_{n=1}^{\infty} \frac{L_n}{n^2} = 7\zeta(3)/4$$

$$\sum_{n=1}^{\infty} \frac{L_n}{n^4} = \left[31\zeta(5) - 14\zeta(2)\zeta(3)\right]/4 \qquad \text{(B5)}$$

Again the process can be continued ad libitum.

Particularly interesting because of its simplicity is the first formula of Eq. (B5). This formula relates directly $\zeta(3)$, the sum over n^{-3}, and the sum over $n^{-2}L_n$.

The second formula of Eq. (B5) is used in this paper to calculate the coefficient E_0 of its set E_μ, see Eq. (C3). For this purpose it is very convenient. On the other hand, our new formulas may not be more convenient than the numerical approach Eq. (B2) if the given set E_μ contain $\log \mu$ directly. An example would be the slowly converging sum

$$\sum_{n=2}^{\infty} \frac{\log n}{n^2} = 0.9375482..$$

which one may calculate either way.

Note that the two sequences of new summation formulas, Eqs. (B4,5), arise solely from the series presentation Eq. (9) for the pressure function $\bar{p}$. No statement about the downwash w is involved, not even a statement that w should be physically meaningful. Rather, the Kutta condition $\bar{p}_{t.e.}=0$ in Eq. (9) leads directly to Eqs. (2),(13),(14) and (15) and thence to Eqs. (B4,5). The salient fact is that the Kutta condition enforces duality between the two sets $C_{2\mu}$ and $C_{2\lambda+1}$.

APPENDIX C

ELEMENTARY SUMS $C_{0,E}$

We have

$$C_{0,E} = -\sum_{1}^{\infty} C_{2\varkappa,E}$$

for the leading constant of the elementary set $E_{\varkappa}$ because of Eq. (2). Thus $C_0 = \zeta(r)$ for the elementary sets $-C_{2\varkappa} = \varkappa^{-r}$, with ζ the Riemann function, Table 2.3. of Ref. (4). For the remaining sets $E_{\varkappa}$ which are used to construct Tables I to VI, we have

$$\sum_{1}^{\infty} \frac{4}{\varkappa(4\varkappa+1)} = 4\left[\psi(5/4) + \gamma\right] = 1.39908526.. \qquad (C1)$$

from 6.3.16, Ref. (4);

$$\sum_{1}^{\infty} \frac{\log^2 \varkappa}{\varkappa^4} = 0.06505816.. \qquad (C2)$$

by means of Eq. (B2);

$$\sum_{1}^{\infty} \frac{L_{\varkappa}}{\varkappa^4} = 1.115624875.. \qquad (C3)$$

from Eq. (B5).

APPENDIX D

PRESSURE DISTRIBUTIONS

The solutions $C_{\lambda,i}$, Fig. 7, can be considered as elementary solutions, defined by their downwash coefficients

$$w_{s,i} = \begin{cases} 1/(s+1)(2s+1) & \text{for } s=i \\ 0 & \text{" } s\neq i \end{cases} \tag{D1}$$

see Eqs. (57) and (17). A given downwash w(y) and its solution can be built up from a sufficient number of such elements.

If we disregard the operator S_1 (as in Eq. (23)) we have $w_s \approx \overline{\pi} C_{2\lambda+1}$ for $\lambda = s$. Hence, if we define

$$\overline{\pi} C_{2\lambda+1} = \begin{cases} 1/(\lambda+1)(2\lambda+1) & \text{for } \lambda = \lambda^* \\ 0 & \text{" } \lambda \neq \lambda^* \end{cases} \tag{D2}$$

we have alternate elements λ^* (= 0,1,2...) which are somewhat related to the elements i. They also can be used to build up any desired solution. It is of some interest to compare the two types of elements.

The downwash distributions $w_i(y)$ were shown in Fig. 7; Fig. D1 shows the $w_{\lambda^*}(y)$. The major difference is that the latter all turn down to - ∞ at the tip. The reason for this is clear from Eq. (13): the solving set $C_{2\mu}$ of w_{λ^*} contains only even-numbered rational elementary se[illegible] $= \mu^{-2r}$. It is evident from Fig. D1 that, by superposing a sufficient number[∅] of elements λ^*, one can approximate a given w(y) closely enough within any given inner range $|y| \leq y_o < 1$. However, in order to achieve w(1) finite, one has to represent the set $E_\mu = \mu^{-3}$, and this requires an infinite number of elements λ^*.

The purpose of the present appendix is to discuss pressure functions $\bar{p}$. We are interested in cases where w(y) is wavy, and are interested in the nature of the pressure distribution over the inner part of the wing span.

∅ In some respect, this corresponds to the procedure of collocation analyses.

From this point of view, the elements i and λ^* are equivalent. Figures D2 and D3 show the cases $\lambda^* = 1$ and $\lambda^* = 3$ (instead of the corresponding cases i = 1,3 simply because the present figures had already been prepared).

Like Fig. 2, Figs. D2 and D3 are relief diagrams, however, the right half-wing is stretched into a rectangle; furthermore, the rectangle is cut at y = 0.9 for better visibility of $\tilde{p}$. (The wing tip point is stretched into a straight line, a "chord" y = 1.0; thus the linear distribution of $\tilde{p}$ over the front part of this "chord" is shown.) A vertical plane through the leading edge of the rectangle is drawn; it shows horizontal lines of constant $\tilde{p}$ (the scale of $\tilde{p}$ is arbitrary) and vertical lines of constant y.

The left half-wing is not shown in Fig. D2. It is shown, unstretched, in Fig. D3, and over it the wavy incidence distribution w(y) is indicated.

The pressure distributions Figs. D2,3 lead to a somewhat unexpected observation of technical interest: while the waviness of the incidence distribution is well reflected in $\tilde{p}$ along the leading edge, this waviness is rapidly damped out along the chord and already at midchord is no longer recognizable. Over the rear part of the wing, the pressure distribution $\tilde{p}$ no longer reflects the waviness of w(y). This stabilizing effect (shown here on an idealized model) must be generally significant for the influence of disturbances of short characteristic spanwise extension. It is, of course, also the mechanism which makes the wave amplitudes in $C_{\ell,i}$ of Fig. 7 smaller than the corresponding amplitudes in w_i.

Another way of describing the mechanism which leads to Fig. D3 in particular is to say that already the vortices which are shed by the front wing create a downwash field which is almost identical with that of the back part of the wing, such that at the back part almost no new vorticity is created. This mechanism, respectively the chordwise distributions of the lift which are shown in Fig. D3, are distinctly different from the assumptions of lifting line theory. Accordingly, lifting line theory cannot be expected to perform adequately for the downwash w_3. In Fig. D4, the curve $C_{\ell,3}$ of Fig. 7 is repeated (one half-wing only, larger vertical scale), and the result of lifting line theory is also shown. Comparison of the two results reminds one of the fact that lifting line predicts the lift coefficient of the planar slender elliptic wing too large by the factor 2. According to Fig. D4, this amplification factor 2 applies also to wings which have a wavy distribution of the wing incidence, supposing of course that the wave lengths are sufficiently small.

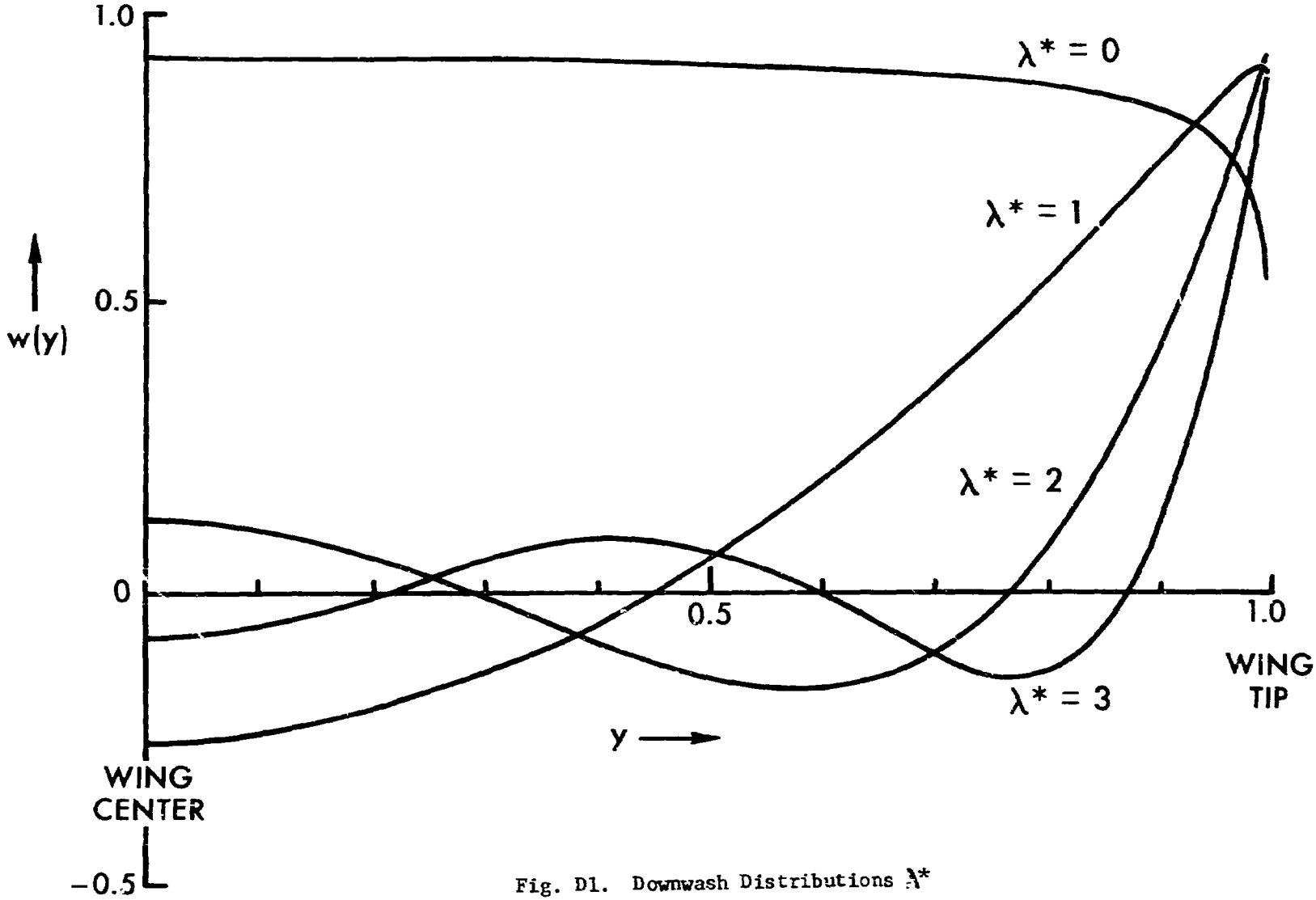

Fig. D1. Downwash Distributions λ^*

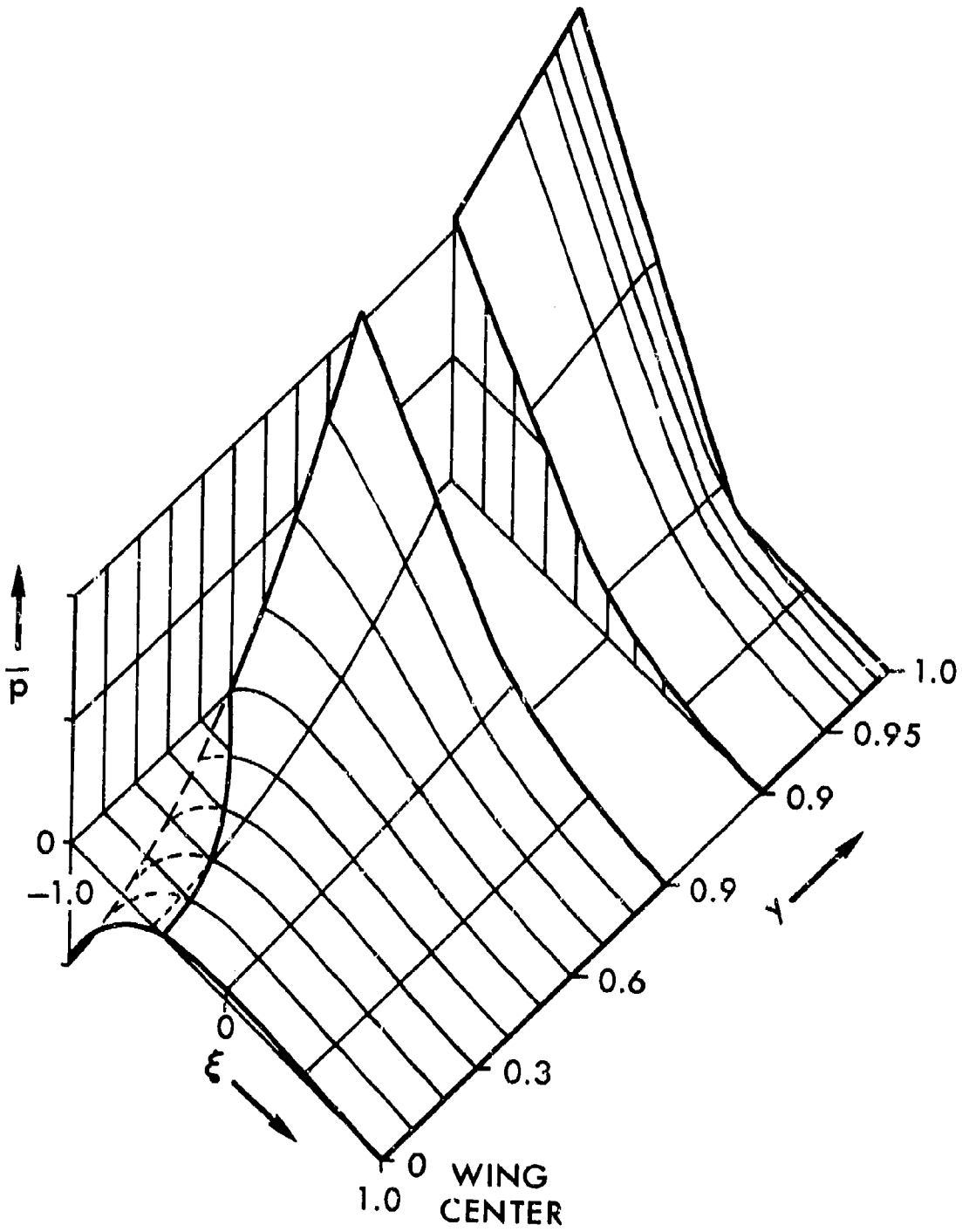

Fig. D2. Pressure Function for $\Lambda^* = 1$

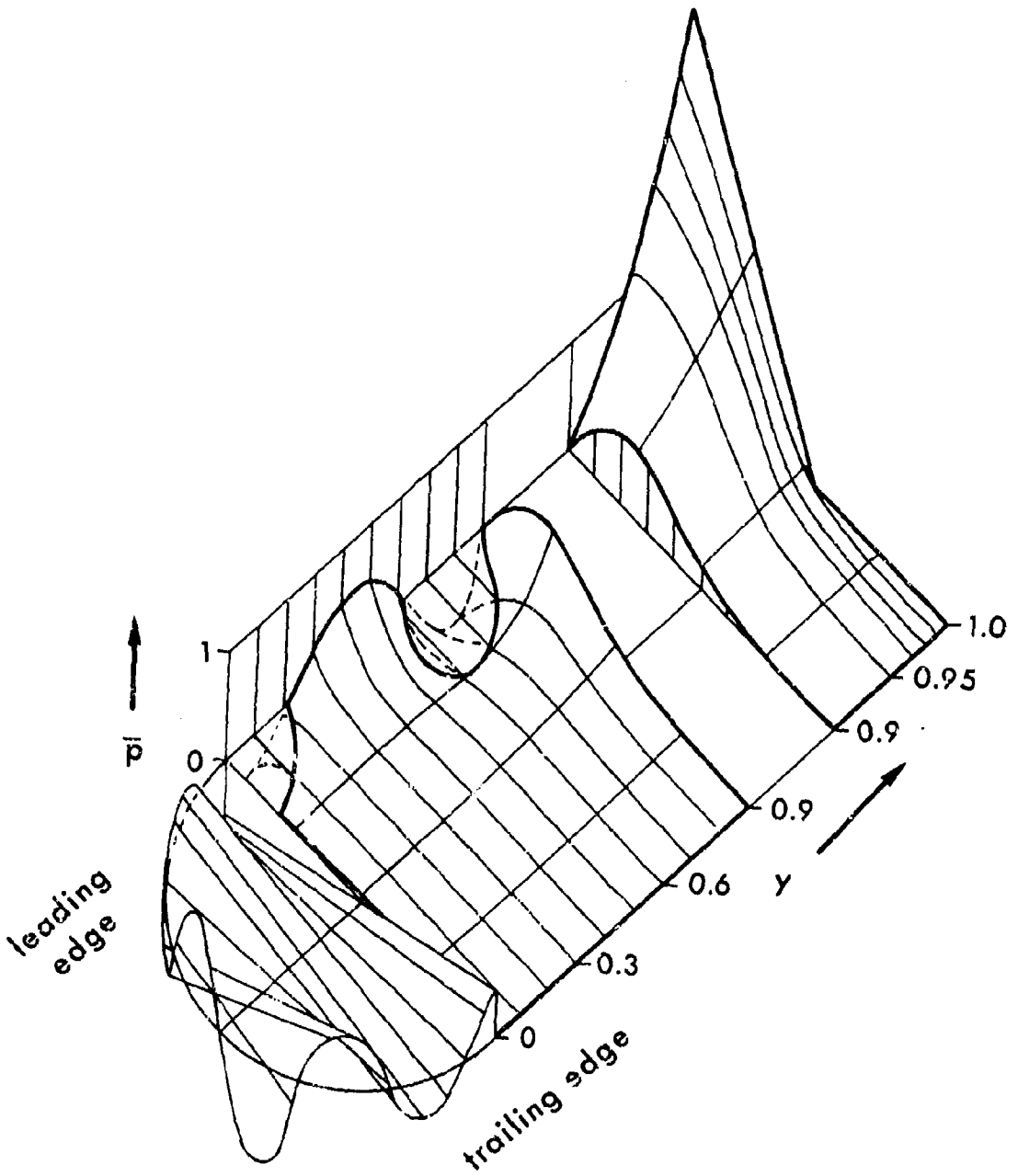

Fig. D3. Pressure Function for $\lambda^* = 3$

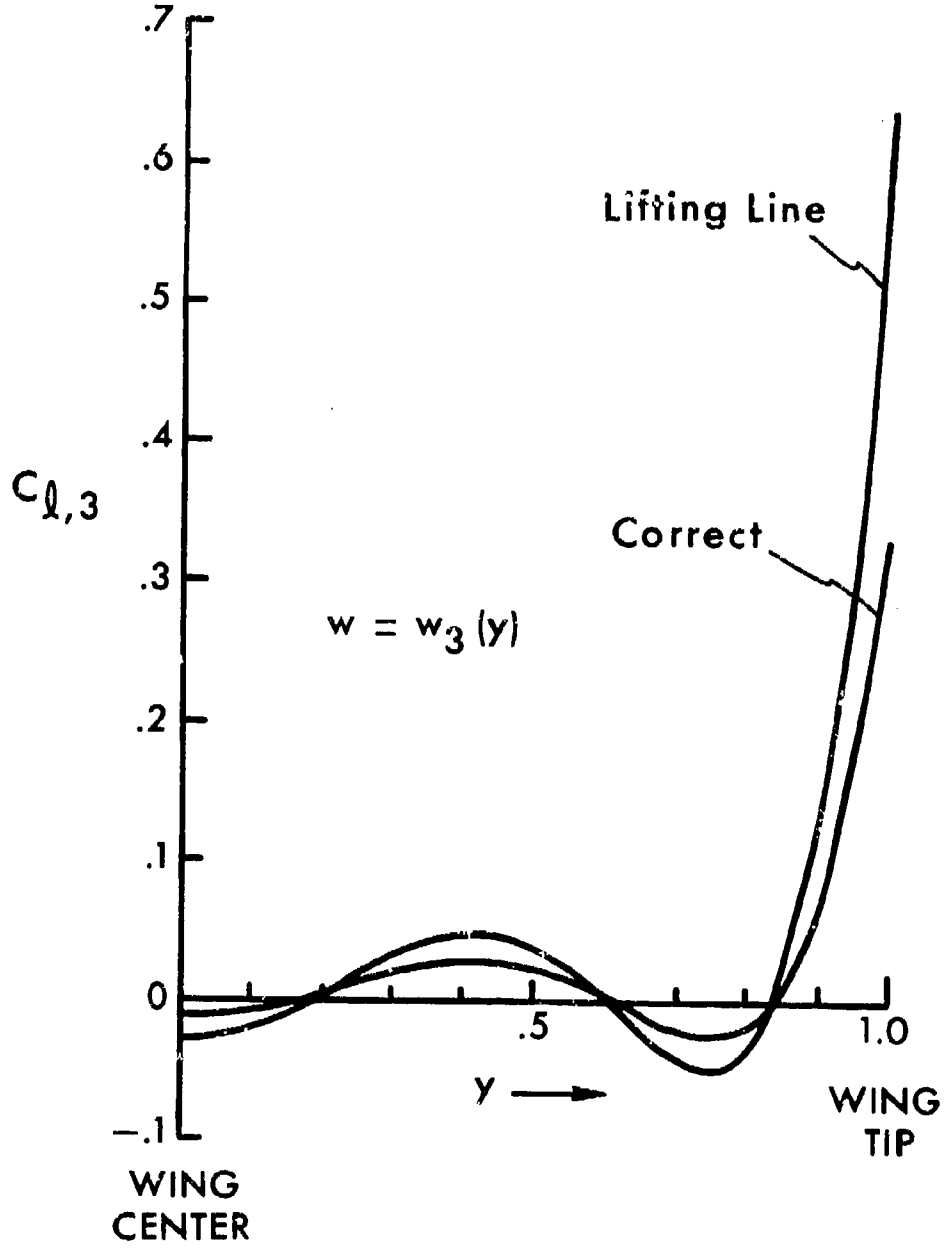

Fig. D4. Comparison of Lifting Line Result with Exact Solution